Shell-Model Theory of Pb^{206}†*‡

WILLIAM W. TRUE,§ *Indiana University, Bloomington, Indiana*

AND

KENNETH W. FORD, *Indiana University, Bloomington, Indiana and Los Alamos Scientific Laboratory, University of California, Los Alamos, New Mexico*

(Received October 11, 1957)

A detailed nuclear shell model calculation of the energy levels and gamma-ray transition rates in Pb^{206} is carried through. For pure singlet two-body forces with the same effective range and strength as for the low-energy two-body system, energy level agreement is good—for 13 known levels, the mean discrepancy between theory and experiment is 0.057 Mev. For singlet forces 75% as strong as for the low-energy two-body system, plus weak coupling to collective vibration, the energy level agreement is somewhat better—the mean discrepancy between theory and experiment is 0.035 Mev per level. In the latter theory, the strength of collective motion is determined from the known Coulomb excitation cross section in Pb^{206}. In either theory, the calculated transition rates are in qualitative accord with experiment, but quantitative agreement is lacking.

Electric quadrupole transition rates are shown to be describable in terms of a neutron effective charge. The effective charge is about $1.15e$ and the same in Pb^{206} as in Pb^{207}. Other calculated quantities in good agreement with experiment are the relative cross sections to final p states in the $Pb^{206}(d,p)Pb^{207}$ reaction and the difference in binding energies of the last neutron in Pb^{206} and Pb^{207}. The results are shown to be insensitive to substantial amounts of triplet-odd force, either attractive or repulsive.

I. INTRODUCTION

IF in a detailed shell model theory of the low-energy properties of a nucleus, one assumes a rigid spherical average potential well and takes account only of a reasonably small number of states, then that theory cannot be expected to have quantitative validity for more than a very small fraction of all medium and heavy nuclei, because of the effects of nuclear deformability. As pointed out by Pryce,[1] nuclei which differ by only a few nucleons from the double-closed-shell nucleus Pb^{208} are among the few for which one might hope that the conventional shell-model theory will lead to a quantitatively correct description. The most striking evidence for the unusual rigidity of Pb^{208} is the energy of its first excited state, 2.6 Mev, which is greater, so far as is known, than the energy of the first excited state of any other nucleus beyond mass number 40. The slow rates of electric quadrupole transitions in the Pb isotopes provide separate evidence for the rigidity of the closed-shell core of 82 protons.[2]

In this paper we select for a detailed application and test of the nuclear shell model the nucleus Pb^{206}. The relevant one-particle states[3] are well known from Pb^{207} and interaction effects only between neutrons and neutrons, not between neutrons and protons, need to be considered. The extension of the calculations to the lower-mass isotopes of Pb is straightforward and is now in progress.

A highly simplified shell theory of the Pb isotopes[2,4,5] has already yielded qualitative agreement with experimental energy levels in the Pb isotopes, and has been a very valuable tool in constructing the complicated decay scheme of Bi^{206}. A more detailed theory, similar to the one in this paper, has also recently been reported by Kearsley.[6] Since her work and ours overlap to some extent, we shall where possible refer to her paper for calculational details. A comparison of our results with those of Kearsley is given in Sec. VB.

A detailed comparison of shell-model theory with experiment may lead in principle to information about the strength, range, and exchange character of the effective two-body force among the extra-shell nucleons, about the presence of many-body forces, about the strength of particle-surface coupling and nuclear deformability, and about the consistency of shell-model energies and shell-model wave functions (i.e., are the shell-model particles real nucleons or only "model-particles"?[7]). The extent to which the present calculations provide such information is discussed in Sec. VIII.

II. EXPERIMENTAL KNOWLEDGE OF THE Pb ISOTOPES

In order to avoid discussions of experimental facts and experimental uncertainties at various places in the remainder of this paper, we summarize here the experimental knowledge about the Pb isotopes which is needed in this work together with our interpretation of the data where ambiguity exists.

Pb^{208}

Known levels of Pb^{208} up to 4 Mev are shown in Table I. The lowest two states may be interpreted as

† This paper is based largely on a Ph.D. thesis submitted to Indiana University in May, 1957, by W. W. True.

* Supported in part by the National Science Foundation.

‡ Supported in part by the U. S. Atomic Energy Commission.

§ Present address: Palmer Physical Laboratory, Princeton, New Jersey.

[1] M. H. L. Pryce, Proc. Phys. Soc. (London) **A65**, 773 (1952).

[2] W. W. True, Phys. Rev. **101**, 1342 (1956).

[3] For convenience we shall usually refer to the neutron holes as "particles." For two-body forces, holes are equivalent to particles to within a constant additive energy. The calculation therefore provides a test of the two-body force assumption.

[4] D. E. Alburger and M. H. L. Pryce, Phys. Rev. **95**, 1482 (1954).

[5] M. H. L. Pryce, Nuclear Phys. **2**, 226 (1956/57).

[6] M. J. Kearsley, Phys. Rev. **106**, 389 (1957); Nuclear Phys. **4**, 157 (1957).

[7] R. J. Eden and N. Francis, Phys. Rev. **97**, 1366 (1955).

TABLE I. Experimental energies in Pb^{208}.

Energy	Spin and parity assignment	Reference
0	0+	a
2.615	3−	a
3.198	5−	a
(3.37)		b
3.475	4−	a
(3.60)		b
3.70	5−	a

[a] Elliott, Graham, Walker, and Wolfson, Phys. Rev. 93, 356 (1954), decay of Tl^{208}.
[b] J. A. Harvey, Can. J. Phys. 31, 278 (1953), $Pb^{207}(d,p)Pb^{208}$.

arising primarily from proton excitation to the configuration $(d_{3/2})^{-1}(h_{9/2})$. This configuration has four states which in order of increasing energy should be[1] 3−, 5−, (4− and 6−). The 3− state is not seen in the $Pb^{207}(d,p)Pb^{208}$ reaction, confirming that it is not due to neutron excitation. Moreover, the lowest excited neutron configuration is expected to be $(p_{1/2})^{-1}(g_{9/2})$, with spins 5− and 4− only. Also among the first group of excited states should be other states of spin 5− and 4− from the proton configuration $(s_{1/2})^{-1}(h_{9/2})$.

From the $Pb^{207}(d,p)$ reaction, Harvey (Table I, reference b) reports states in Pb^{208} at 3.37 and 3.60 Mev. These may be additional states not seen in the decay of Tl^{208}. The energy resolution in his experiment is poor, however, and it is also possible to interpret his single broad peak as a superposition of the three states seen by Elliott *et al.* (Table I, reference a) at 3.198, 3.475, and 3.70 Mev. It is reasonable to assume that these 4− and 5− states, even if primarily due to proton excitation, have sufficient admixtures of neutron excitation to be observed in the (d,p) experiment.

In the absence of detailed calculations or of a more definitive (d,p) experiment, however, we make the following assumptions: (1) The first two excited states in Pb^{208} are due primarily to proton excitation. (2) The energy difference between the ground state neutron configuration $(p_{1/2})^2$ and the lowest state of the excited configuration $(p_{1/2})(j)$ is about 3.3 Mev, where j represents the next neutron level above $p_{1/2}$, probably $g_{9/2}$. Since the interaction energy difference between $(p_{1/2})^2$ and $(p_{1/2})(j)$ is calculated to be at most about 0.7 Mev, the intrinsic level spacing across the shell between j and $p_{1/2}$ is assumed to be at least 2.4 Mev.

There is no evidence for a 2+ state in Pb^{208} below 4 Mev. There is no strong evidence against it, however, except below about 2.5 Mev, which may be taken as a lower limit for the collective phonon excitation energy in Pb^{208}.

Pb^{207}

Known energy levels of Pb^{207} up to 4.6 Mev are shown in Table II. The first five levels (to 2.35 Mev) are interpreted as single neutron hole states. The lowest state which can be interpreted as arising from the excitation of a $p_{1/2}$ neutron to the next shell is at 2.71 Mev. This is consistent with the foregoing conclusion for Pb^{208} that the neutron excitation energy to the next shell is at least 2.4 Mev. Up to 2.4 Mev, there is no evidence for states due to proton excitation. Since levels beyond 2.4 Mev have been excited only by (d,p) reactions, proton excitation states beyond 2.4 Mev would not have been seen. (However, the two states near 4.5 Mev may be interpreted as strongly mixed states of proton and of neutron excitation.)

The $E2$ transition rate from the first excited state to the ground state is[8]

$$T_{E2}(\tfrac{5}{2}\rightarrow\tfrac{1}{2})=(6.9\pm1.6)\times10^{9}\ \text{sec}^{-1}. \quad (1)$$

This corresponds to a reduced transition rate,[9] $B_e(2)=(92\pm22)e^2\times10^{-52}$ cm^4, where e=electron charge. The interpretation of this transition rate in terms of weak collective motion have been considered in a previous paper,[2] and will be discussed further in Sec. VC.

Pb^{206}

Experimental energies in Pb^{206} are summarized in Table III from three sources—the experimental studies of Alburger on the conversion electrons and gamma rays following the decay of Bi^{206}, the work of Day, Johnsrud, and Lind on inelastic scattering of neutrons by Pb^{206}, and the work of Harvey on the reaction $Pb^{207}(d,t)Pb^{206}$. For convenience, theoretical configuration assignments are included in the table. For levels excited in the (d,t) reaction, these assignments are partially implied by experiment, i.e., these levels must be of the form $(p_{1/2}j)$. This implies in particular that the level reported by Harvey at approximately 3.03 Mev is probably distinct from the levels reported by Alburger and Pryce at 3.017 Mev and 3.125 Mev. Two spin and parity assignments differ from those given by Alburger and Pryce[4] for theoretical reasons to be discussed in Sec. IVA: the level at 3.017 Mev is changed from 6− to 5− and the level at 3.125 Mev is changed from 5+ to 6+.

TABLE II. Experimental energies in Pb^{207}.

Energy	Spin and parity assignment	Interpretation as neutron level	Reference
0	1/2−	$(p_{1/2})^{-1}$	a
0.570	5/2−	$(f_{5/2})^{-1}$	a
0.90	3/2−	$(p_{3/2})^{-1}$	a
1.634	13/2+	$(i_{13/2})^{-1}$	a
2.35	7/2−	$(f_{7/2})^{-1}$	a
2.71	(9/2+?)	$(p_{1/2})^{-2}(g_{9/2})$?	b
3.61	(11/2+?)	$(p_{1/2})^{-2}(i_{11/2})$?	b
4.37	?	$(p_{1/2})^{-2}(j)$[c]	b
4.62	?	$(p_{1/2})^{-2}(j)$[c]	b

[a] D. E. Alburger and A. W. Sunyar, Phys. Rev. 99, 695 (1955); N. H. Lazar and E. D. Klema, Phys. Rev. 98, 710 (1955). Decay of Bi^{207}.
[b] McEllistrem, Martin, Miller, and Sampson (to be published), $Pb^{206}(d,p)Pb^{207}$ (see reference 11). Similar, but somewhat less accurate values given by J. A. Harvey [Can. J. Phys. 31, 278 (1953)].
[c] The symbol j refers to an excited neutron level, possibly $g_{7/2}$ or $d_{5/2}$.

[8] P. H. Stelson and F. K. McGowan, Phys. Rev. 99, 127 (1955).
[9] For notation, see, e.g., B. J. Alder *et al.*, Revs. Modern Phys. 28, 432 (1956).

TABLE III. Experimental energies in Pb^{206}.

Energy	Spin and parity assignment	Probable dominant configuration	Reference
0	0+	$(p_{1/2})^2$	e
0.803	2+	$(p_{1/2}f_{5/2})$	e
1.341	3+	$(p_{1/2}f_{5/2})$	e
1.34[a]	3+(0+)	$(p_{1/2}f_{5/2})_3,(f_{5/2})_0^2$	f
1.45	2+	$(p_{1/2}p_{3/2})$	f
1.37[b]		$(p_{1/2}j)$	g
1.684	4+	$(f_{5/2})^2$	e
1.71	1+	$(p_{1/2}p_{3/2})$	g
1.73	1+(2+)	$(p_{1/2}p_{3/2})_1,(f_{5/2})_2^2$	f
1.83	(2+)	$(f_{5/2})_2^2$	f
1.998	4+	$(p_{3/2}f_{5/2})$	e
2.15	1+(2+,3+,0+)	$(p_{3/2})_0^2,(p_{3/2}f_{5/2})_{1,2,3}$	f
2.200	7−	$(p_{1/2}i_{13/2})$	e
2.22[c]		$(p_{1/2}j)$	g
2.385	6−	$(p_{1/2}i_{13/2})$	e
2.526	3−	$[(d_{3/2})^{-1}(h_{9/2})]_{\text{proton}}$	e
2.783	5−	$(f_{5/2}i_{13/2})$	e
3.017	5−	$(p_{3/2}i_{13/2})$	e
3.03[d]	(3+,4+)	$(p_{1/2}f_{7/2})$	g
3.125	6+	$(f_{5/2}f_{7/2})$	e
3.280	5−	$[(d_{3/2})^{-1}(h_{9/2})]_{\text{proton}}$	e
3.404	5−	$[(s_{1/2})^{-1}(h_{9/2})]_{\text{proton}}$	e

[a] This level, excited by inelastic neutron scattering, may be the same as the 3+ level, but is also consistent with a 0+ assignment. It could be either or a superposition of both.
[b] This level, observed with poor energy resolution in the (d,t) reaction, is probably a superposition of the 3+ level at 1.34 Mev, the 2+ level at 1.45 Mev, and possibly also a 0+ level.
[c] This level, observed with poor energy resolution in the (d,t) reaction, is probably a superposition of the 7− level at 2.200 Mev and the 6− level at 2.385 Mev.
[d] This level was reported as probably a doublet. It is probably a superposition of the 3+ and 4+ levels arising from the configuration $(p_{1/2}f_{7/2})$ and distinct from the other levels indicated in the neighborhood of 3 Mev.
[e] D. E. Alburger and M. H. L. Pryce, Phys. Rev. **95**, 1482 (1954). Decay of Bi^{206}.
[f] Day, Johnsrud, and Lind, Bull. Am. Phys. Soc. Ser. II, **1**, 56 (1956). $Pb^{206}(n,n'\gamma)$. We are indebted to R. Day and D. Lind for more detailed information concerning their experimental results.
[g] J. A. Harvey, Can. J. Phys. **31**, 278 (1953). $Pb^{207}(d,t)Pb^{206}$.

The measured $E2$ transition rate in Pb^{206} from the first excited state to the ground state is[8]

$$T_{E2}(2\rightarrow 0)=(103\pm 25)\times 10^{9}\ \text{sec}^{-1}. \qquad (2)$$

This corresponds to a reduced transition probability, $B_e(2)=(250\pm 62)e^2\times 10^{-52}$ cm^4. The interpretation of this transition rate in terms of weak collective motion was considered in a previous paper,[2] but the surface tension derived there was in error by a factor $2^{\frac{1}{3}}$. The numerical correction and further modification arising from configuration mixing are discussed in Sec. VC.

Pb^{204}

Known levels of Pb^{204} below 2.2 Mev are given in Table IV. No detailed theoretical analysis of this nucleus will be presented in this paper, but it will be possible to make a quantitative statement about the spacing of the two 4+ levels.

Transition Rates

Bi^{206} *Beta Decay*

Bi^{206} decays predominantly by K capture to two 5 states in Pb^{206} at 3.280 Mev and 3.404 Mev, probably by first forbidden transitions from a parent 6+ state.[4] A 6+ state in Pb^{206} at 3.125 Mev is also populated, and weak transitions to other high-spin states in Pb^{206} (e.g., 5− states at 2.783 and 3.017 Mev) are also possible. The theoretical significance of the selection of final states in the Bi^{206} decay has been discussed by Alburger and Pryce.[4]

Pb^{206} *Gamma Transitions*

The experimental knowledge of gamma transition rates in Pb^{206} is summarized in Table V. The measured K-electron intensities[4] are translated to gamma intensities by means of the finite-nucleus K-conversion coefficients of Sliv and Band (reference c in Table V). For comparison with theoretical branching ratios only the gamma transition rates are needed. However, in order to test also the over-all consistency of the decay scheme, we correct for conversion in shells higher than K and list also the total transition rates. The L/K ratios are taken from point-nucleus conversion coefficients evaluated by Rose, and we arbitrarily set $(L+M+\cdots)/K=1.20L/K$ for all transitions. The notation 6−, 2 means the second state of spin six and odd parity, in order of increasing energy.

This table differs in several respects from the similar table in reference 4. (a) Finite-nucleus conversion coefficients are used. (b) The transitions are all assumed to be of a pure multipole type. With one or two possible exceptions, $E2$ radiation is not expected to compete with $M1$ radiation in this nucleus when the latter is allowed. The fact that $E2$ is known to compete with $M1$ in other nuclei may be explained by the fact that in most other nuclei collective effects are much stronger and l-forbiddenness is more prevalent. In Pb^{206}, $E2$ radiation is not strongly enhanced and $M1$ radiation is (with a few exceptions) not strongly inhibited. We therefore tentatively assume in Table V that $M1$ radiation is dominant in all transitions where it is allowed. (c) We have not adjusted any of the total transition rates in order to obtain consistency with the decay scheme. (d) We have indicated several expected transitions which could be masked by stronger transitions with nearly the same energy. For example, a weak $E2$ transition of 878 kev from 5−, 4 to 3−, 1 is expected, in analogy with the observed 754-kev transition as-

TABLE IV. Experimental energies in Pb^{204}.

Energy	Spin and parity assignment	Half-life	Reference
0	0+		a
0.899 Mev	2+	$<6\times 10^{-10}$ sec	a
1.274	4+	0.27 μsec	a
1.563	4+		a
1.818	(4+)		b
1.945	(5+)		b
2.066	(5+)		b
2.186	9−	68 min	a

[a] Herrlander, Stockendal, McDonell, and Bergström, Nuclear Phys. **1**, 643 (1956).
[b] A. R. Fritsch, University of California Radiation Laboratory Report UCRL-3452, June, 1956 (unpublished).

TABLE V. Transition rates in Pb^{206}.

No.[a]	Transition energy (kev)	Assumed parent	Assumed daughter	type	Relative K-electron intensity[b] I_K	Conversion coeff.[c] α_K	Relative gamma intensity[b] I_γ	Assumed[d] $(L+M+\cdots)/K$	Relative total transition rate
1	184.1	6−,1	7−,1	$M1$	28	1.35	20.7	0.20	54.3
2	234.3	5−,2	5−,1	$M1$	0.24	0.68	0.35	0.20	0.64
3	262.8	5−,3	5−,2	$M1$	2.1	0.50	4.2	0.20	6.7
4	343.4	4+,1	3+,1	$M1$	$6.6-x_1$	0.240	$27.5-4.17x_1$	0.20	$35.4-5.37x_1$
	(341.8)	6+,1	5−,1	$E1$	x_1	0.0178	$56.2x_1$	0.20	$57.4x_1$
5	386.0	5−,4	5−,2	$M1$	0.13	0.176	0.74	0.20	0.90
6	398.1	5−,1	6−,1	$M1$	1.76	0.160	11.0	0.20	13.1
7	497.1	5−,3	5−,1	$M1$	1.37	0.091	15.1	0.20	16.7
8	516.1	7−,1	4+,1	$E3$	1.95	0.0487	40.0	0.73	43.4
9	537.5	3+,1	2+,1	$M1$	2.08	0.074	28.1	0.20	30.6
10	620.6	5−,4	5−,1	$M1$	0.27	0.0505	5.35	0.20	5.7
11	632.2	5−,2	6−,1	$M1$	0.21	0.0485	4.33	0.20	4.6
12	657.3	4+,2	3+,1	$M1$	0.084	0.0435	1.93	0.20	2.0
13	803.3	2+,1	0+,1	$E2$	0.85	0.0080	106	0.27	107
14	880.5	4+,1	2+,1	$E2$	$0.48-x_2$	0.0067	$71.6-149x_2$	0.26	$72.2-150x_2$
	(878.0)	5−,4	3−,1	$E2$	x_2	0.0067	$149x_2$	0.26	$150x_2$
15	895.1	5−,3	6−,1	$M1$	0.32	0.0193	16.6	0.20	17.0
16	1018.8	5−,4	6−,1	$M1$	0.11	0.0140	7.86	0.20	8.0
17	1098.6	5−,1	4+,1	$E1$	0.029	0.00177	16.4	0.18	16.4
18	1596.3	5−,3	4+,1	$E1$	0.0054	0.00094	5.74	0.18	5.8
19	1719.7	5−,4	4+,1	$E1$	0.029	0.00083	34.9	0.18	34.9
20	123.6	5−,4	5−,3	$M1$	0.069	4.10	0.0168	0.20	0.10
21	202.5	7−,1	4+,2	$E3$	0.020	0.410	0.049	5.8[e]	0.185
22	313.6	4+,2	4+,1	$M1$	0.14	0.305	0.46	0.20	0.63
23	739.9	6+,1	6−,1	$E1$	0.011	0.00363	3.03	0.18	3.0
24	753.9	5−,3	3−,1	$E2$	0.0074	0.0091	0.81	0.28	0.82
25	816.3	5−,2	7−,1	$E2$	$0.0025-x_3$	0.0077	$0.325-130x_3$	0.27	$0.33-131x_3$
	(∼816)	6−,2	7−,1	$M1$	x_3	0.0245	$40.8x_3$	0.20	$42x_3$
26	841.7	3−,1	4+,1	$E1$	0.0050	0.00287	1.74	0.18	1.75
27	1405.2	5−,4	4+,2	$E1$	0.0020	0.00114	1.75	0.18	1.75
28	107.2	6+,1	5−,2	$E1$	$0.23-x_4$	0.300	$0.77-3.33x_4$	0.23	$1.05-4.56x_4$
	(∼107)	6+,1	6−,2	$E1$	x_4	0.300	$3.33x_4$	0.23	$4.56x_4$
...	...	...	...	...	...	...	...	...	...
29	662	2+,2	2+,1	$M1$			4		4
30	1460	2+,2	0+,1	$E2$			1		1
31	1730	1+,1	0+,1	$M1$					
32	1830	2+,3	0+,1	$E2$					
33	1350	1+,2(2+,4)	2+,1	$M1$					

[a] The first 28 transitions are numbered as by Alburger and Pryce (reference 4). Transitions 29–33 are additional transitions observed by Day, Johnsrud, and Lind (reference f in Table III).
[b] The K-electron intensities are taken from reference 4. The normalization of intensities for transition 29 and 30 is unrelated to the normalization of transitions 1–28.
[c] The K-conversion coefficients are taken from L. Sliv and I. Band, University of Illinois Report 57 ICC K1, April, 1957 (unpublished).
[d] The L/K ratios are evaluated by interpolation among values distributed by M. E. Rose (Oak Ridge National Laboratory) based on point nucleus calculations. We arbitrarily set $(L+M+\cdots)/K=1.20(L/K)$.

signed from 5−, 3 to 3−, 1. This transition could be masked by the strong 880.5-kev transition. We assign K-electron intensities x_i (unknown) to four such possible masked transitions. Several other transitions, not masked, are expected, and will be discussed in Sec. IVB.

As a test of the consistency of the decay scheme, we present in Table VI the total transition intensities to and from each state, taken from Table V. The x_i are unknown intensities defined above, and β indicates an unknown population of the state by β decay. Aside from possible errors in the decay scheme, lack of perfect consistency in Table VI can arise from a number of sources: (a) uncertainty in measured K-electron intensities, which are stated to be[4] about 15% for energies above 250 kev and up to 30% for energies below 250 kev; (b) uncertainty in K-conversion coefficients and in L/K ratios; (c) possible $E2-M1$ mixing in some transitions. In view of the uncertainties, adequate consistency for all levels can be obtained by setting all of the x_i equal to zero and the total β intensity equal to 107. The strongly populated states (lowest levels of 0+, 2+, 3+, 4+, 5−, 6−, and 7−) then give consistency to

TABLE VI. Consistency test of transition intensities.

State	To	From
0+,1	107	...
2+,1	$102.8-150x_2$	107
3+,1	$37.4-5.37x_1$	30.6
3−,1	$0.82+150x_2$	1.75
4+,1	102.9	$107.6-5.37x_1-150x_2$
4+,2	1.94	2.6
5−,1	$23.0+57.4x_1$	29.5
5−,2	$8.65-4.56x_4$	$5.57-131x_3$
5−,3	$0.1+\beta$	47.0
5−,4	β	$51.4+150x_2$
6−,1	45.7	54.3
6−,2	$4.56x_4$	$42x_3$
6+,1	β	$4.05+57.4x_1$
7−,1	$65.6-89x_3$	43.6

within about 20%. Some improvement can be obtained by setting $\chi_1 \sim 0.2$, $\chi_2 \sim 0.007$. It remains an open question whether the uncertain transitions indicated by $\chi_1, \chi_2, \chi_3, \chi_4$ do or do not occur with appreciable probability.

In order to clarify the rather complicated decay scheme and aid in reading the information in Tables V and VI, we present in Fig. 1 in the form of a Grotrian diagram all of the known energy levels and transitions in Pb^{206} [excluding the levels assigned from the $Pb^{207}(d,t)$ reaction], the spin and parity assignments being those of Table III.

$Pb^{206}(d,p)Pb^{207}$ *Cross Sections*

Since (d,p) reactions can provide a method of measuring the degree of configuration mixing in nuclear states,[10] and do so for Pb^{206}, the recent $Pb^{206}(d,p)$ experiment of McEllistrem *et al.*[11] with 11-Mev deuterons, is of interest. Their relevant results are indicated in Table VII. Higher excited states than those indicated in the table are also seen, but do not concern us here.

Absolute Binding Energies

The $Pb^{206}(n,\gamma)Pb^{207}$ energy release is[12] 6.734 ± 0.008 Mev. The $Pb^{207}(n,\gamma)Pb^{208}$ energy release[12] is 7.380 ± 0.008 Mev. In the shell model, the magnitudes of these separation energies depend on the total depth and size of the nuclear potential. Only the difference of these two numbers, 0.65 Mev, can be predicted by the present calculation. We shall call this difference $\Delta^2 B$ (second difference of total binding energies). It is compared with theory in Sec. VI.

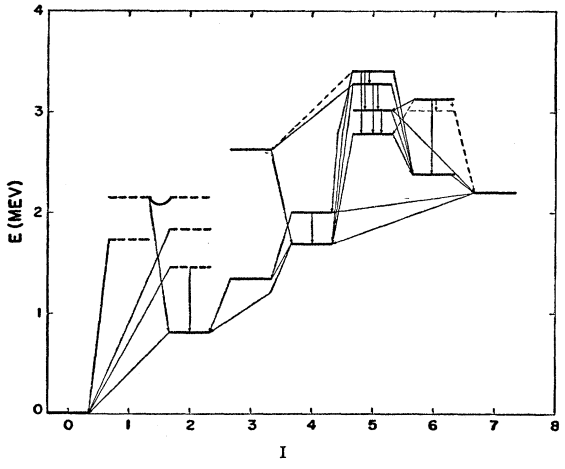

FIG. 1. Known energy levels and transitions in Pb^{206}. The energies and transitions follow almost uniquely from experiment. Some of the spin and parity assignments may be incorrect, however. Dashed energy levels are those seen in inelastic neutron scattering. Solid energy levels are those seen in the decay of Bi^{206}. Dashed transitions are those which may exist in the decay of Bi^{206} but be masked by other more intense transitions with nearly identical energies. All levels with $I \leq 4$ are of even parity unless otherwise marked. All levels with $I \geq 5$ are of odd parity unless otherwise marked.

TABLE VII. $Pb^{206}(d,p)Pb^{207}$ experiment.[a]

Energy of final state	Configuration assignment	Angle of peak cross section	Maximum cross section (mb/steradian)	Total cross section
0	$(p_{1/2})^{-1}$	65°	0.31	2.01
0.570	$(f_{5/2})^{-1}$	89°	0.058	0.371
0.90	$(p_{3/2})^{-1}$	64°	0.087	0.62
1.634	$(i_{13/2})^{-1}$	...	...	~0
2.35	$(f_{7/2})^{-1}$	...	...	~0
2.71	$(p_{1/2})^{-2}(g_{9/2}?)$	103°	1.51	...

[a] See McEllistrem, Martin, Miller, and Sampson, reference 11.

III. CALCULATIONS WITH SINGLET FORCES

A. Assumptions and Parameters

Our initial guiding philosophy in the present work was to avoid as far as possible the adjustment of any parameters to fit the properties of the nucleus under study, Pb^{206}, and to do this by assuming for the direct two-body force between pairs of extra nucleons a force with the same low-energy properties as the force observed in the isolated two-body system. This assumption leads to good agreement with energy levels in Pb^{206}. Some knowledge of the sensitivity of the results to the assumption is provided by Kearsley's work[6] and by comparison of our results with hers (Sec. VB). As shown in Sec. VC3, however, even better agreement with experiment may be obtained by a more self-consistent treatment in which collective coupling is included, but in which the strength of the direct two-body force is reduced. We discuss first (Secs. III and IV) the treatment of the problem and the results, ignoring the effect of collective coupling on energies.

The introduction of a repulsive core in the two-body force leads to practical difficulties in a shell-model calculation which have not yet been surmounted. The center-of-mass energy for two-body scattering within the nucleus is less than about 80 Mev, and the repulsive core is not playing a dominant role in the scattering. It is of some significance, however. Brueckner[13] estimates that total cross sections calculated with a monotonic attractive potential and calculated with the "best" potential including a repulsive core[14] differ by about 30% at a laboratory energy of 100 Mev, or matrix elements of the potential by about 15%. The average scattering energy for the outer nucleons is less than this amount. Although the use of a potential without repulsive core in a shell model

[10] J. French and J. Raz, Phys. Rev. **104**, 1411 (1956).

[11] McEllistrem, Martin, Miller, and Sampson (to be published). We are indebted to these workers for providing us with the results of their experiments before publication.

[12] D. M. Van Patter and W. Whaling, Revs. Modern Phys. **26**, 402 (1954).

[13] K. A. Brueckner (private communication).

[14] Gammel, Christian, and Thaler, Phys. Rev. **105**, 31 (1957), and subsequent work to be published. We are indebted to these authors for providing us with the most recent, unpublished results of their analyses.

calculation is almost forced upon one by practical necessity, it is probably not a serious source of error in the calculation. Some previous calculations[15] have indicated that the matrix elements of potentials with the same effective range and scattering length are very insensitive to changes of the radial dependence of the potential. We have therefore chosen arbitrarily the Gaussian radial dependence of the potential, which is convenient for calculations.

Since we are concerned only with the neutron-neutron force in this calculation, we have to deal only with the singlet-even and triplet-odd exchange types. The singlet-even force is known to be much stronger than the triplet-odd force,[14] and we therefore adopt pure singlet forces for our principal calculations. The effect of triplet forces is examined less completely as a perturbation on the singlet results (Sec. VA), and the effect of triplet forces may also be inferred from the results of Kearsley (Sec. VB). We take for the singlet potential

$$V=V_0\exp(-r^2/\beta^2), \tag{3}$$

with $V_0=-32.5$ Mev and $\beta=1.85\times10^{-13}$ cm. This potential has an effective range, $r_{os}=2.65\times10^{-13}$ cm,[16] and a bound state at zero energy.

For the radial wave functions we choose harmonic oscillator functions,[17]

$$\psi_{nlm}\sim r\exp(-\tfrac{1}{2}r^2/b^2)r^lL_{n+l+\frac{1}{2}}^{l+\frac{1}{2}}(r^2/b^2)Y_{lm}(\theta,\varphi), \tag{4}$$

where $L_q^p(x)$ is an associated Laguerre polynomial.[18] The shape of the average central potential in Pb is probably very different from a harmonic oscillator. However a potential as different as a square well has wave functions which differ very little from oscillator wave functions provided the two radial constants are suitably adjusted. The p and f neutrons which occurs in the Pb isotopes are associated with the $n=5$ harmonic oscillator level, and the i neutrons with the $n=6$ level. We adjust the nuclear size parameter b in (4) so that the classical turning point of the $n=5$ level (for zero angular momentum) is equal to a suitable nuclear radius, $\bar{r}$. This requires that $(13/2)\hbar\omega=\frac{1}{2}M\omega^2\bar{r}^2$, or, since $b^2=\hbar/M\omega$, that $b^2=\bar{r}^2/13$. We determine $\bar{r}$ by assuming that Pb^{206} may be represented by a potential of the form,

$$V(r)=V_0[1+\exp(\alpha r-\alpha R)]^{-1}, \tag{5}$$

with $V_0=-40$ Mev, $\alpha=2.02\times10^{13}$ cm^{-1}, and $R=1.33A^{\frac{1}{3}}\times10^{-13}$ cm.[19] The radius of this potential for a particle with 10-Mev binding is taken to be $\bar{r}$. This criterion gives $\bar{r}=8.40\times10^{-13}$ cm$=1.42A^{\frac{1}{3}}\times10^{-13}$ cm, and implies $b=2.33\times10^{-13}$ cm. This process of determining b is illustrated in Fig. 2. Slightly better compensation for the fact that the potential is not harmonic could be made by choosing a different value of b for each particle level. This refinement considerably complicates the calculation and has not been made. The relevant parameter measuring the "shortness" of the range of the two-body force is the ratio $\beta/b=0.79$.

The unperturbed positions of the one-particle levels are taken to be the empirical positions of the levels in Pb^{207} (Table II).

In this way the parameters of the calculation are determined, independently of the properties of Pb^{206}. One parameter does remain to be adjusted, the absolute binding energy difference between Pb^{206} and Pb^{207}. We normalize the computed energies to give agreement between theory and experiment for the lowest 3+ level in Pb^{206}. However, it is shown in Sec. V that the absolute energy agrees with theory to within 0.05 Mev.

B. Calculational Methods

Our evaluation of the matrix elements of the two-body potential between the various relevant two-particle states in Pb^{206} followed calculational methods developed by Talmi[17] and by Kennedy.[20] After our calculations were completed, better methods of Slater integral evaluation were developed by Thieberger,[21] whose method is similar to Kennedy's but simpler in practice, and by Konopinski,[22] whose formula for the

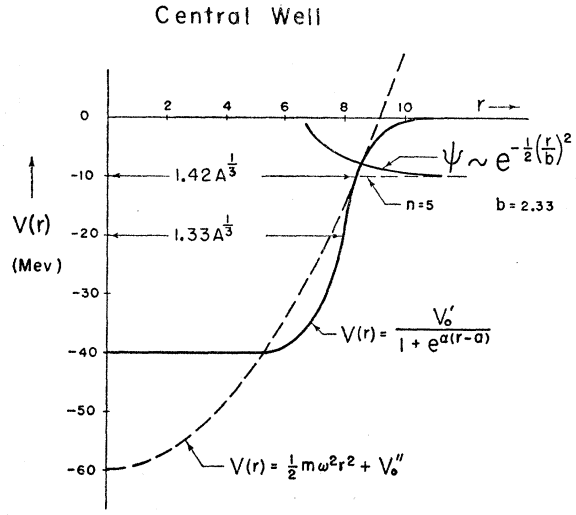

FIG. 2. Method used to determine radial parameter of harmonic oscillator wave functions. The parameters of the Saxon potential (solid line) are those determined in the analysis of proton scattering, and the two potentials are made to agree at an energy of -10 Mev. The radius r and parameter b are given in units of 10^{-13} cm.

[15] C. Levinson and K. Ford, Phys. Rev. **99**, 792 (1955).
[16] H. A. Bethe and P. Morrison, *Elementary Nuclear Theory* (John Wiley and Sons, Inc., New York, 1956), second edition, p. 94.
[17] I. Talmi, Helv. Phys. Acta **25**, 185 (1952).
[18] W. H. Shaffer, Revs. Modern Phys. **16**, 245 (1944).
[19] Ross, Mark, and Lawson, Phys. Rev. **102**, 1613 (1956).
[20] J. M. Kennedy (private communication). We are indebted to Dr. Kennedy for informing us of his work and supplying us with useful tables of coefficients $C_k^s(m,n)$ [see Eq. (9)] before publication.
[21] R. Thieberger, Nuclear Phys. **2**, 533 (1957).
[22] E. J. Konopinski (private communication).

Slater integral with Gaussian two-body force is a great simplification. We therefore outline here only briefly the calculational method which is employed.

To be evaluated are the interaction matrix elements,

$$V_{\text{int}}={}_a\langle j_1(1)j_2(2)I\,|\,V\,|\,j_1'(1)j_2'(2)I\rangle_a, \tag{6}$$

where $|j_1(1)j_2(2)I\rangle_a$ is an antisymmetric two-particle wave function in the j-j coupling representation. We transform first to the L-S representation[23] and then obtain formulas for the interaction matrix elements in terms of Slater integrals, Racah coefficients and coefficients $C_{lkl'}$ (integrals over three Legendre polynomials), exactly as worked out by Racah[24] for the electrostatic interaction, taking advantage, of course, of the exchange nature of the present interaction. The integrand of the Slater integral R^k is a product of four radial wave functions and the quantity $v_k(r_1,r_2)$ defined by

$$V(|\mathbf{r}_1-\mathbf{r}_2|)=\sum_k v_k(r_1,r_2)P_k(\cos\theta_{12}). \tag{7}$$

Explicit expansion of the integrand in powers of r makes it possible to express the Slater integral as a sum of terms, each of which contains an integral of the form:

$$f_k(m,n)=(2k+1)^{-1}\int x_1^{m+2}x_2^{n+2}\times\exp[-(x_1^2+x_2^2)]v_k(bx_1,bx_2)dx_1dx_2, \tag{8}$$

where $x_{1,2}=r_{1,2}/b$ [b is defined by Eq. (4)]. The double integrals $f_k(m,n)$ may then be expanded in terms of the Talmi single integrals[17] I_s:

$$f_k(m,n)=(\tfrac{1}{2}\pi)^{\frac{1}{2}}\sum_{s=0}^{m+n}C_k{}^s(m,n)I_s, \tag{9}$$

where s takes on only even values, and

$$I_s=\int x^sV(bx)\exp(-\tfrac{1}{2}x^2)x^2dx. \tag{10}$$

The major amount of labor in this method of Slater integral evaluation is the calculation of the Kennedy coefficients[20] $C_k{}^s(m,n)$. Once they are tabulated, however, the labor required for additional shell model calculations is greatly reduced.[25] In order to evaluate the $C_k{}^s(m,n)$, one substitutes into Eq. (8),

$$v_k(bx_1,bx_2)=\tfrac{1}{2}(2k+1)\int_1^1 V(bx)P_k(\theta_{12})d\theta_{12}. \tag{11}$$

One then transforms from the $\mathbf{x}_1$, $\mathbf{x}_2$ coordinates to the center-of-mass and relative coordinates, $\mathbf{X}=\frac{1}{2}(\mathbf{x}_1+\mathbf{x}_2)$ and $\mathbf{x}=\mathbf{x}_2-\mathbf{x}_1$. It is possible to integrate over $\mathbf{X}$, and the resulting expression for $f_k(m,n)$ is of the form (9). Because of the fact that $f_k(m,n)=f_k(n,m)$ and because certain angular factors multiplying the $f_k(m,n)$ vanish, it is necessary to evaluate the coefficients $C_k{}^s(m,n)$ only for $n\leq m$, $k\leq n$, and m, n, and k either all odd or all even.

A serious disadvantage of this method of calculation, aside from the considerable labor required to evaluate the $C_k{}^s(m,n)$ is that the sum (9) involves very large cancellations and it is necessary to evaluate the $C_k{}^s(m,n)$ and the I_s to much higher accuracy than is required in the final answer. The Talmi integrals I_s, it should be noted, are very simple for the Gaussian potential (3):

$$I_s=V_0[(s+1)!!][1+2b^2/\beta^2]^{-\frac{1}{2}(s+3)}(\tfrac{1}{2}\pi)^{\frac{1}{2}}, \tag{12}$$

where $s!!\equiv s(s-2)(s-4)\cdots$.

The number of levels of given spin and parity which were included in the energy diagonalization was chosen in a somewhat arbitrary way to include all states below about 3.4 Mev. The effect of individual higher states on the lowest energy state of each spin and parity is small (but not necessarily the sum of the effect of all higher states). Our results should therefore be more accurate for the lower energy state than for the higher, and for the lower spin states than the higher. A consistent treatment including states above about 3.4 Mev is in any case not feasible at present, since unknown states of proton excitation or of neutron excitation to the next shell occur beyond this energy. In the diagonalization process[26] we included four 0+ states, two 1+ states, five 2+ states, three 3+ states, three 4+ states, two 5− states, three 6− states, three 7− states, and two 8− states. Some other states of spins 1 through 5 and one state of spin 9 were also included in lowest order (diagonal matrix elements only). Only a single 4− state, a single 6+ state, and a single 9− state, are predicted.

IV. RESULTS WITH SINGLET FORCES

A. Energy Level Results

The calculated energy levels are given in Table VIII and in Fig. 3. The energy levels are normalized to agree with experiment for the 3+ level at 1.341 Mev, which has both a small diagonal energy shift and a small degree of configuration mixing. The unrenormalized zero of energy is the unperturbed position of $(p_{\frac{1}{2}})^2$. The renormalization requires that 0.811 Mev be added to all calculated energies. This brings the theoretical ground-state position into very close agreement with experiment. Of the total of 0.8-Mev total level shift of $(p_{\frac{1}{2}})^2$, about half is from the diagonal energy contribution, and about half from configuration mixing. In the simplified theory of Pryce,[4] this extra shift due to

[23] Transformation coefficients given by G. Racah [Physica **16**, 651 (1950)] and in a neater form by Arima, Horie, and Tanabe [Progr. Theoret. Phys. (Japan) **11**, 143 (1954)]. Our phases agree with the latter authors.

[24] G. Racah, Phys. Rev. **62**, 438 (1942).

[25] Tables of the coefficients $C_k{}^s(m,n)$ for most combinations of m, n, and k values from 0 through 12 (and all associated s values) are available from the authors upon request.

[26] The matrices were diagonalized on the IBM 650 computer at Indiana University. We are grateful to Dr. Keith Howell for making available to us his code for finding the eigenvalues and eigenvectors of symmetric matrices.

TABLE VIII. Energy levels and eigenfunctions calculated for singlet forces in Pb^{206}.

Energy (Mev)	Eigenfunctions				
$I=0+$	$(p_{1/2})^2$	$(f_{5/2})^2$	$(p_{3/2})^2$	$(i_{13/2})^2$	
0.011	0.8653	0.3077	0.3765	−0.1216	
1.232	−0.4138	0.8755	0.1794	−0.1736	
2.058	−0.2821	−0.3273	0.9006	−0.0476	
3.156	0.0204	0.1781	0.1228	0.9761	
$I=1+$	$(p_{1/2}p_{3/2})$	$(p_{3/2}f_{5/2})$			
1.711	1	0			
2.281	0	1			
3.731	$(f_{5/2}f_{7/2})$				
$I=2+$	$(p_{1/2}f_{5/2})$	$(p_{1/2}p_{3/2})$	$(f_{5/2})^2$	$(p_{3/2}f_{5/2})$	$(p_{3/2})^2$
0.804	0.7229	−0.6017	0.2168	0.1509	0.2134
1.253	0.6538	0.7347	0.0016	0.0438	−0.1757
1.754	−0.1784	0.1540	0.9695	0.0673	0.0059
2.221	−0.1313	0.0752	−0.1046	0.9805	0.0695
2.465	−0.0305	0.2623	−0.0463	−0.0971	0.9585
3.497	$(p_{3/2}f_{7/2})$				
3.653	$(f_{5/2}f_{7/2})$				
$I=3+$	$(p_{1/2}f_{5/2})$	$(p_{3/2}f_{5/2})$	$(p_{1/2}f_{7/2})$		
1.341	0.9987	0.0471	−0.0189		
2.236	−0.0478	0.9981	−0.0383		
3.135	0.0171	0.0392	0.9991		
3.731	$(f_{5/2}f_{7/2})$				
3.977	$(p_{3/2}f_{7/2})$				
$I=4+$	$(f_{5/2})^2$	$(p_{3/2}f_{5/2})$	$(p_{1/2}f_{7/2})$		
1.705	0.6688	0.7021	−0.2444		
1.963	0.7416	−0.6533	0.1526		
2.979	0.0525	0.2834	0.9576		
3.548	$(f_{5/2}f_{7/2})$				
3.859	$(p_{3/2}f_{7/2})$				
$I=4-$					
3.001	$(f_{5/2}i_{13/2})$				
$I=5-$	$(f_{5/2}i_{13/2})$	$(p_{3/2}i_{13/2})$			
2.894	0.8126	−0.5828			
3.097	0.5828	0.8126			
$I=5+$					
3.731	$(f_{5/2}f_{7/2})$				
4.061	$(p_{3/2}f_{7/2})$				
$I=6-$	$(p_{1/2}i_{13/2})$	$(f_{5/2}i_{13/2})$	$(p_{3/2}i_{13/2})$		
2.433	0.9998	0.0152	−0.0137		
2.989	−0.0158	0.9991	−0.0387		
3.323	0.0131	0.0389	0.9992		
$I=6+$					
3.100	$(f_{5/2}f_{7/2})$				
$I=7-$	$(p_{1/2}i_{13/2})$	$(f_{5/2}i_{13/2})$	$(p_{3/2}i_{13/2})$		
2.217	0.9705	0.1873	−0.1520		
2.907	−0.2134	0.9604	−0.1792		
3.267	0.1124	0.2063	0.9720		
$I=8-$	$(f_{5/2}i_{13/2})$	$(p_{3/2}i_{13/2})$			
2.980	1	0			
3.341	0	1			
$I=9-$					
2.628	$(f_{5/2}i_{13/2})$				

mixing had to be postulated in order to obtain agreement with experiment for the ground state.

In order to illustrate the role of configuration mixing, we include in Fig. 3 both the results in lowest order (diagonal matrix elements only), and the results after mixing. Ambiguity of spin and parity assignments exists for a few levels, and the reasons for our assignments are given in Sec. IVB.

As is evident in Fig. 3, agreement between theory and experiment for energy level positions is generally excellent. For the ground state, the lowest 2+ state, and the splitting of the two 4+ states, configuration mixing is very important in producing the agreement with experiment. Also all levels in which configuration mixing is not very important agree closely with experiment—these are the 1+, 3−, 6−, 6+, and 7− levels. We conclude that the over-all strength of the two-body potential which we use is nearly correct, i.e., that the potential strength which fits two body scattering and the potential strength acting between extra nucleons in the shell model (in Pb^{206}!) are nearly equal. This conclusion will be somewhat altered when the effect of collective coupling (or, equivalently, the effect of many higher configurations) is included. As will be shown in Sec. VA, we cannot conclude that the exchange character we have chosen is correct, because the energy level results are insensitive to the exchange mixture.

Theoretical level positions disagree with experiment only for the higher 2+ levels and the 5− levels. The latter disagreement can be easily understood and indeed is expected. Since proton excitation states occur in Pb^{208} at 2.6 Mev (3−) and at 3.2 Mev (5−), one expects that states of the same character should occur at nearly the same energy in Pb^{206}, and these predicted levels are indicated in Fig. 3 by crosshatched bands. No other levels except these two and those arising from the two neutron holes are expected below about 3.4 Mev. Above this energy, other states of more complicated type are expected. The 3− "core-excited" state does not interact with any near-lying neutron hole states. However, the 5− core excited state is close to the two 5− neutron hole states and should perturb them. In fact, the lowest observed 5− state is somewhat below the lowest predicted 5− state, which was calculated ignoring this perturbation, as would be expected. One must also account for the fact that (according to our assignments) four 5− states are observed and only three predicted. Since the beta decay proceeds strongly and about equally to the upper two and weakly or not at all to the lower two, we assume that the upper two are predominantly of core-excited type, enabling a one-particle beta transition to occur from Bi^{206}, and the lower two are predominantly neutron-hole type, associated with the two such predicted levels, to which beta decay would be strongly inhibited. There are several different ways in which 5− core-excited levels may be formed: protons, $(d_{3/2})^{-1}h_{9/2}$ and $(s_{1/2})^{-1}h_{9/2}$; neutrons $(p_{1/2})^{-2}(f_{5/2})^{-1}g_{9/2}$.

We do not have any simple explanation for the failure of agreement between theory and experiment for the upper 2+ states. We note, however, that the agree-

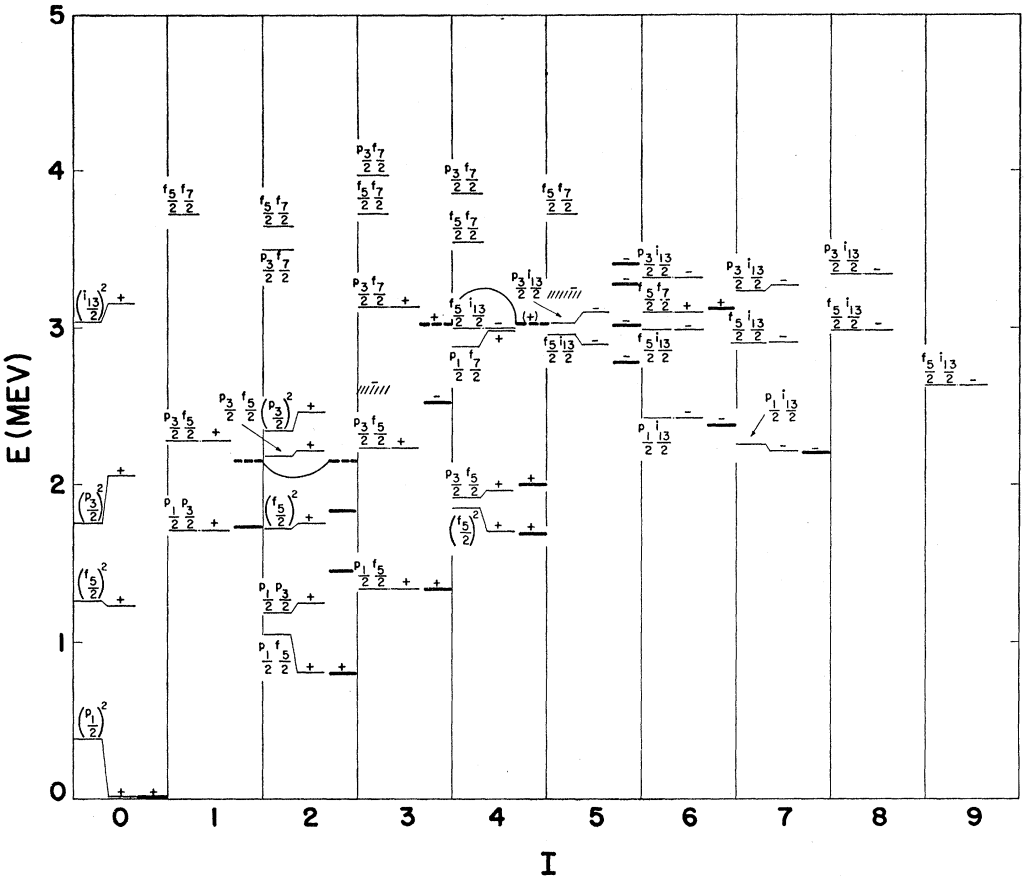

FIG. 3. Energy levels of Pb^{206}. For each spin, the first column gives the energy levels calculated in lowest order with singlet forces, together with the configuration assignment. The second column gives the theoretical energy levels calculated by exact diagonalization of the energy matrix for the lowest few states of each spin and parity. The third column gives the empirical levels. The positions of all of the energy levels are reasonably certain, but the spin and parity assignment of a few levels are uncertain.

ment would be somewhat better for a shorter-range force (see comparison with zero-range results below). Substantially improved agreement is also brought about by the inclusion of weak collective coupling.

Comparison with Zero-Range-Force Results

Our diagonal-element results without configuration mixing fit the experimental energies about as well as the zero-range results of Alburger and Pryce.[4] These two calculations have in common that the forces are pure singlet, but differ in that the range of our force is finite and of theirs, zero, and that we calculate the radial integrals while they estimated them. It is interesting to observe, however, that our diagonal matrix elements are in rather close agreement with those of Alburger and Pryce, except for the $(f^2)_0$ and $(i^2)_0$ configurations for which the zero range matrix elements are considerably larger in magnitude than the finite-range matrix elements, and the $(p^2)_2$ configuration, for which the zero-range matrix element is smaller than the finite-range matrix element. Table IX compares our diagonal matrix elements with those of Pryce and Alburger for some sample configurations.

An experimental level at 1.46 Mev shows the greatest discrepancy from theory, if it is correctly assigned as 2+. Predicted 2+ levels are at 1.25 and 1.75 Mev. We have found that a decrease of about 35% in the diagonal element for p^2, $L=2$, which brings this matrix element into agreement with the zero-range matrix element, with no other change, somewhat improves agreement between theory and experiment. For $I=2$, the predicted levels are changed from 0.80 to 0.86 Mev (experiment 0.803); from 1.25 to 1.37 (experiment 1.46); from 1.75 to 1.76 (experiment 1.83); for the 2.22 level, no change; and from 2.47 and 2.57.

Certain simple rules characteristic of short-range singlet forces are evident in Fig. 3 and Table VIII. Levels with spin and parity both even or both odd ($l_1+l_2+I=$even) have larger energy shifts and larger mixing than levels with even (odd) spin and odd (even) parity ($l_1+l_2+I=$odd). It is in fact a well-known property of all even-even nuclei that levels of the latter type are rarely seen among the low-lying states. For

the levels of a given configuration $(j_1 j_2)$, either the lowest spin-value, $|j_1-j_2|$, or the highest spin-value, j_1+j_2, will be lowest in energy, whichever satisfies the condition $l_1+l_2+I=$ even. Any level I of the configuration will lie lower (higher) than its two neighbors $I\pm1$ if it does (does not) satisfy the same condition. For example, the odd-parity configuration $f_{5/2}i_{13/2}$ has six states whose spin-values, in order of increasing energy, are 9, 7, 5 (5, 7 after mixing) 8, 6, 4.

The differences in the present results and the lowest order results with a zero-range force[4] are only in quantitative detail. The qualitative features of the simple theory are maintained.

B. Wave Function Results

Our calculated eigenfunctions for singlet forces are shown in Table VIII. Also included for completeness are some levels not included in the diagonalization process, which are designated as being single pure j-j configurations. The absence of mixing is of course not to be taken seriously for these levels. For $I=1+$ and $8-$, however, the singlet off-diagonal matrix elements vanish identically, and the indicated purity of the states is of significance. It will be observed that the calculated degree of mixing is very different for different spins. It is great for $0+$, $2+$, and $4+$, small for $3+$, and zero for $1+$. It is considerably greater for $7-$ than for $6-$.

The agreement of calculated energy levels with experiment, especially the extra depression of the ground state due to configuration mixing and the splitting of the two strongly-mixed $4+$ states, indicates that the degree of configuration mixing is roughly correct. Transition rates are a much more sensitive test of the eigenfunctions, however, and we discuss below the gamma-ray transition rates and the $Pb^{206}(d,p)Pb^{207}$ cross sections.

1. Gamma Transition Rates

The transition rate for gamma rays of a given multipolarity λ is [27,28]

$$T(\lambda)=\frac{8\pi(\lambda+1)}{\lambda[(2\lambda+1)!!]^2}\frac{1}{\hbar}\left(\frac{\Delta E}{\hbar c}\right)^{2\lambda+1}B(\lambda), \qquad (13)$$

where ΔE is the transition energy. The reduced transition probability $B(\lambda)$ is given by

$$B(\lambda)=(2I'+1)^{-1}|\langle\Gamma I\|M_\lambda\|\Gamma' I'\rangle|^2, \qquad (14)$$

in which I is the *final* spin, I' the *initial* spin, and Γ and Γ' represent all other quantum numbers characterizing the states. The double-bar matrix element is defined as by Racah,[24] and M_λ represents the multipole operator, to be defined below for $M1$ and $E2$ transitions.

[27] J. M. Blatt and V. F. Weisskopf, *Theoretical Nuclear Physics* (John Wiley and Sons, Inc., New York, 1952), p. 595.

[28] A. Bohr and B. Mottelson, Kgl. Danske Videnskab. Selskab, Mat.-fys. Medd. **27**, No. 16 (1953).

TABLE IX. Comparison of some finite-range diagonal matrix elements with zero-range matrix elements of Alburger and Pryce.

Configuration	Matrix elements in Mev: Finite range	Zero range
$(p_{1/2})^2 0+$	−0.427	−0.40
$(f_{5/2})^2 0+$	−0.685	−1.20
$(p_{3/2}f_{5/2})1+$	0	0
$(p_{1/2}f_{5/2})2+$	−0.329	−0.36
$(p_{1/2}p_{3/2})2+$	−0.520	−0.32
$(p_{3/2})^2 2+$	−0.260	−0.16
$(f_{5/2})^2 2+$	−0.235	−0.27
$(p_{3/2}f_{5/2})2+$	−0.094	−0.10
$(p_{1/2}f_{5/2})3+$	−0.037	0
$(p_{3/2}f_{5/2})3+$	−0.046	0
$(f_{5/2})^2 4+$	−0.101	−0.11
$(p_{3/2}f_{5/2})4+$	−0.364	−0.34

The usual multipole operators are one-particle operators, i.e.,

$$M_\lambda=\sum_i M_\lambda(i), \qquad (15)$$

summed over the particles, with the $M_\lambda(i)$ equal for all neutrons and equal for all protons. The operator for collective $E2$ transitions is not of this form. However, as will be proved in Sec. VC, for weak collective motions, the $E2$ rate is exactly the same as for a particle transition, in which the particles carry an effective charge determined by the strength of collective coupling (and by $\langle r^2\rangle_{Av}$ for the particle state in question, which we take to be about the same for all states). This result holds for arbitrary mixing of the states. We may therefore use the form (15) for the particle $M1$ transitions and the collective $E2$ transitions, which are of interest in Pb^{206}. We will not calculate the $E1$ and $E3$ rates.

Let the pure j-j coupling states of the shell model be labeled by β and γ and expand the initial and final states,

$$|\Gamma' I'\rangle=\sum a_\gamma'|\gamma I'\rangle, \quad |\Gamma I\rangle=\sum a_\beta|\beta I\rangle. \qquad (16)$$

Then the reduced double-bar matrix element in (14) becomes

$$\langle\Gamma I\|M_\lambda\|\Gamma' I'\rangle=\sum_{\beta,\gamma}a_\beta^* a_\gamma'\langle\beta I\|M_\lambda\|\gamma I'\rangle. \qquad (17)$$

For operators of the type (15), the two-particle matrix element[29] in (17) between j-j states may be expanded in terms of one-particle matrix elements (antisymmetrized two-particle states are assumed):

Case A, $j'\neq j$, $j''\neq j$:

$$\langle jj'I\|M_\lambda\|jj''I\rangle=[(2I+1)(2I'+1)]^{\frac{1}{2}}\times[(-1)^{\lambda+j'-j-I'}W(j'Ij''I';j\lambda)\langle j'\|M_\lambda\|j''\rangle+(-1)^{\lambda+j'-j-I}W(jIjI';j'\lambda)\langle j\|M_\lambda\|j\rangle\delta_{j'j''}], \qquad (18)$$

where j is shorthand for the quantum numbers nlj. For Case B, $j'=j$, $j''\neq j$, the second term in (18) vanishes and the first must be multiplied by $2^{\frac{1}{2}}$. For Case C, $j=j'=j''$, the two terms in (18) are equal and (18) requires no modification.

[29] Equation (17) is general, but we here specialize to the two-particle statesi n Pb^{206}.

We now define the $M1$ and $E2$ operators in terms of their one-particle matrix elements. Let the $M1$ operator be designated by M_1 and the $E2$ operator by Q_2. Then

$$\langle j\|M_1\|j\rangle=[(3/4\pi)j(j+1)(2j+1)]^{\frac{1}{2}}g_j(e\hbar/2Mc), \quad (19)$$

where g_j is the g factor for the state lj;

$$\langle j\|M_1\|j'\rangle=(-1)^{j-l-\frac{1}{2}}(g_l-g_s)\times\{(3/4\pi)[2l(l+1)/(2l+1)]\}^{\frac{1}{2}}(e\hbar/2Mc), \quad (20)$$

for $l=l'$, $j\neq j'$; and

$$\langle j\|Q_2\|j'\rangle=e_{\text{eff}}\langle r^2\rangle[(5/4\pi)(2j+1)]^{\frac{1}{2}}(j2\tfrac{1}{2}0|j2j'\tfrac{1}{2}), \quad (21)$$

where e_{eff} is the effective charge, $\langle r^2\rangle$ is the matrix element of r^2 between initial and final state,[30] and $(j_1j_2m_1m_2|j_1j_2jm)$ is a Clebsch-Gordan coefficient in the notation of Condon and Shortley.[31] The selection rules on (21) are $l=l'$ or $l'\pm2$, $|j-j'|\leq2$.

For convenience we define dimensionless reduced transition probabilities B'. For $M1$ transitions, let

$$B_m'(1)=(4\pi/3)(e\hbar/2Mc)^{-1}B_m(1). \quad (22)$$

For $E2$ transitions, let

$$B_e'(2)=(4\pi/5)[e_{\text{eff}}\langle r^2\rangle]^{-2}B_e(2). \quad (23)$$

For the neutron transitions in Pb^{206}, we take $e_{\text{eff}}=1.15e$ (see Sec. VC), and $\langle r^2\rangle=(3/5)(1.20A^{\frac{1}{3}}\times10^{-13}\text{ cm})^2$. Then the transition rates are

$$\begin{aligned}T(M1)&=4.25\times10^{12}(\Delta E)^3B_m'(1)\text{ sec}^{-1},\\ T(E2)&=0.595\times10^{12}(\Delta E)^5B_e'(2)\text{ sec}^{-1},\end{aligned} \quad (24)$$

if the transition energy ΔE is expressed in Mev. We have used the above set of formulas to calculate the $M1$ and $E2$ transition rates in Pb^{206}, using the eigenfunctions given in Table VIII. The results for the levels of greatest interest are given in Table X, and predicted branching ratios are compared with experiment (for gamma transitions only, not including conversion).

With a few exception where the $M1$ transition is strongly inhibited (none of these exceptions are among the observed transitions), the transitions between states of the same parity, $\Delta I=0$ or 1, are all calculated to be nearly pure $M1$. The predicted lack of mixing is easy to understand qualitatively. The $\Delta l=0$ selection rule for the $M1$ transitions is satisfied for almost all of the transitions, and the $E2$ transitions are not strongly enhanced (the known $E2$ rates in the Pb isotopes are in fact slower than in almost all other nuclei where $E2$ rates have been measured). In general $M1$ inhibition or $E2$ enhancement is required to permit the $E2$ radiation to compete with or dominate the $M1$ radiation. We have therefore calculated the gamma-ray intensities from the measured K-electron intensities assuming pure multipole radiation.

A rough measure of the reliability of the theoretical transition rates is provided by the "cancellation factor" C in Table X. The transition matrix element for mixed states is a sum of terms, each of which is the product of an amplitude of a component of the initial state, an amplitude of a component of the final state, and the transition matrix element between these components [Eq. (17)]. Let P be the magnitude of the sum of all of the positive terms, and N the magnitude of the sum of all of the negative terms. The total transition rate is then proportional to $(P-N)^2$. The cancellation factor is defined by

$$C=|P-N|/(P+N).$$

For $C\ll1$, the calculated transition rate is very sensitive to small changes in the eigenfunctions. For $C\sim1$, the calculated rate is insensitive to small changes in the eigenfunctions and is therefore more reliable.

Spin and Parity Assignments

The agreement between theory and experiment for gamma branching ratios is only fair. Only order-of-magnitude trust in the theoretical transitions rates is required, however, in order to draw useful conclusions from them. One such conclusion, discussed above, is that most of the $M1$ transitions are nearly pure. Another conclusion is that certain spin and parity assignments can be made.

In the Alburger-Pryce decay scheme we have altered two level assignments. One of these is the 6+, 1 level, of the $f_{5/2}f_{7/2}$ configuration, which was called 5+ by them, owing to the assignment $h_{9/2}$ instead of $f_{7/2}$ to the 2.35-Mev level in Pb^{207}. Either is consistent with the decay scheme, but only one with theory. This level is populated in the beta decay, which is reasonable if the parent Bi^{206} has a 6+ ground state. No spin and parity change make this apparently an allowed transition, but it should be strongly inhibited because the dominant configurations in parent and daughter states differ in the quantum numbers of more than one particle.

The other altered assignment is our 5−, 2 level at 3.017 Mev, which was called 6− by Alburger and Pryce. Either assignment agrees well with theory in energy. However, our 6−, 2 level is predicted to decay to the 7−, 1 level forty times more strongly[32] than to the 6−, 1 level, while the experimental level at 3.017-Mev decays only one twelfth as strongly to the 7−, 1 level as to the 6−, 2 level. For the 6− assignment, the discrepancy factor between theory and experiment for the ratio of these two transitions is about 500. For the 5− assignment, the discrepancy factor is about 5. The latter discrepancy seems quite tolerable, since the 5− eigenfunctions are not expected to be very accurate (owing to the nearby core-excited levels of the same spin and parity).

We have also made assignments for the levels dis-

[30] Since $e_{\text{eff}}\sim[\langle r^2\rangle]^{-1}$ (see Sec. VC), (21) is in fact independent of $\langle r^2\rangle$. It is nevertheless convenient to write it in this way for most direct comparison with proton transition rates.

[31] E. U. Condon and G. H. Shortley, *The Theory of Atomic Spectra* (Cambridge University Press, New York, 1951), p. 75.

[32] Throughout this section, intensities refer to gamma-ray intensities only, not including conversion.

TABLE X. Gamma-ray transition rates in Pb^{206}, based on pure singlet forces.

Parent state	Energy (Mev)	Daughter state	Energy (Mev)	Transition energy (Mev)	Type	Rate (10^{12} sec^{-1})	Cancellation factor, C	Relative rate	Experiment
0+,2	(1.23)	2+,1	0.80	(0.43)	$E2$	0.000315	0.147	···	
0+,3	(2.06)	1+,1	1.73	(0.33)	$M1$	2.50	1.00	1	
		2+,1	0.80	(1.26)	$E2$	0.0028	0.0324	0.0011	
0+,4	(3.16)	1+,1	1.73	(1.43)	$M1$	2.78	1.00	1	
		1+,2	(2.15)	(1.01)	$M1$	~0	···	~0	
		2+,1	0.80	(2.36)	$E2$	1.38	0.767	0.50	
1+,1	1.73	0+,1	0	1.73	$M1$	51.1	0.528	1	1
		0+,2	(1.23)	(0.50)	$M1$	1.01	1.00	0.020	
		2+,1	0.80	0.93	$M1$	1.25	0.333	0.024	
		2+,2	1.46	0.27	$M1$	0.080	0.494	0.0016	
1+,2	(2.15)	0+,1	0	(2.15)	$M1$	~0	···	~0	
		0+,2	(1.23)	(0.92)	$M1$	~0	···	~0	
		1+,1	1.73	(0.42)	$M1$	~0	···	~0	
		2+,1	0.80	(1.35)	$M1$	43.5	1.00	1	(1)
		2+,2	1.46	(0.69)	$M1$	3.45	1.00	0.079	
		3+,1	1.34	(0.81)	$E2$	0.0341	0.887	0.00078	
2+,1	0.803	0+,1	0	0.803	$E2$	0.103	1.00	···	($T=0.103\pm0.025$)
2+,2	1.46	0+,1	0	1.46	$E2$	0.00158	0.0286	0.0058	0.25
		2+,1	0.80	0.66	$M1$	0.272	0.220	1	1
2+,3	1.83	0+,1	0	1.83	$E2$	0.0071	0.0812	0.042	1
		2+,1	0.80	1.03	$M1$	0.170	0.239	1	
		2+,2	1.46	0.37	$M1$	0.0205	0.650	0.121	
		3+,1	1.34	0.49	$M1$	0.00089	0.209	0.0052	
2+,4	(2.15)	0+,1	0	(2.15)	$E2$	0.00253	0.0402	0.00016	
		1+,1	1.73	(0.42)	$M1$	0.230	1.00	0.014	
		2+,1	0.80	(1.35)	$M1$	16.2	0.644	1	(1)
		2+,2	1.46	(0.69)	$M1$	1.62	0.651	0.100	
		2+,3	1.83	(0.32)	$M1$	0.0098	0.425	0.00060	
		3+,1	1.34	(0.81)	$M1$	3.36	0.988	0.207	
3+,1	1.341	2+,1	0.803	0.538	$M1$	0.0282	0.362	···	
3+,2	(2.15)	2+,1	0.80	(1.35)	$M1$	4.33	0.433	0.62	
		2+,2	1.46	(0.69)	$M1$	0.866	0.695	0.123	
		2+,3	1.83	(0.32)	$M1$	0.0209	0.890	0.0030	
		3+,1	1.34	(0.81)	$M1$	7.03	0.990	1	
		4+,1	1.68	(0.47)	$M1$	0.822	0.937	0.117	
4+,1	1.684	2+,1	0.803	0.881	$E2$	0.167	0.941	1	$1-2.1x_2$
		3+,1	1.341	0.343	$M1$	0.113	0.379	0.68	$0.38-0.058x_1$
4+,2	1.998	2+,1	0.803	1.195	$E2$	0.0789	0.316	0.065	
		3+,1	1.341	0.657	$M1$	1.22	0.535	1	1
		4+,1	1.684	0.314	$M1$	0.313	1.00	0.26	0.24
5−,1	2.783	6−,1	2.385	0.398	$M1$	0.451	0.984	···	
5−,2	3.017	5−,1	2.783	0.234	$M1$	0.0542	0.798	0.016	0.081
		6−,1	2.385	0.632	$M1$	3.33	0.967	1	1
		7−,1	2.200	0.817	$E2$	0.0328	0.717	0.0098	$0.075-30x_3$
6−,1	2.385	7−,1	2.200	0.185	$M1$	0.0223	0.670	···	
6−,2	(3.017)	5−,1	2.783	(0.234)	$M1$	0.097	0.937	0.32	
		6−,1	2.385	(0.632)	$M1$	0.0078	0.602	0.026	
		7−,1	2.200	(0.817)	$M1$	0.301	0.875	1	
		7−,2	(2.91)	(0.11)	$M1$	0.0167	0.978	0.055	
7−,1	2.200	4+,1	1.684	0.516	$E3$	···	1.00	1	1
		4+,2	1.998	0.202	$E3$	···	1.00	0.00056	0.00123
7−,2	(2.91)	6−,1	2.39	(0.52)	$M1$	0.123	0.902	1	
		7−,1	2.20	(0.71)	$M1$	0.0697	0.224	0.57	

covered by Day *et al.* (Table III, reference f) at 1.46, 1.73, 1.83, and 2.15 Mev. The 1.46 level is observed to branch 80% to the 2+, 1 level at 0.803 Mev and 20% to the ground state. We make a 2+ assignment, and calculate transition rates using the eigenfunction for the 2+ state predicted at 1.25 Mev. The prediction is a dominant decay of 2+, 2 to 2+, 1, with only 1 part in 2000 decaying to the ground state. However, it will be observed in Table X that the cancellation factor for the ground-state decay is very small, $C=0.0286$. Not very large changes in the eigenfunction would therefore be required in order to increase the ground-state transition rate by a factor of several hundred. Since the theoretical and experimental energies do not agree well in this case, the eigenfunction cannot be expected to be very good.

The state at 1.73 Mev is observed to decay to the ground state. Its energy and decay are consistent only with the lowest 1+ level, predicted at 1.71 Mev. A 20% branch of the decay of this state to the 2+, 1 level at 0.803 Mev is predicted, but not yet seen. The 2.15-Mev state is observed to decay to the 2+, 1 level. This is inconsistent with a 0+ assignment since the 0+, 3 level, predicted near this energy, should decay almost 100% to the 1+, 1 level. It is consistent, however, either with the 1+, 2 level, predicted to decay nearly 100% to the 2+, 1 level, or with the 2+, 4 level, predicted to decay about 90% to the 2+, 1 level.

The level at 1.83 Mev decays to the ground state. A 2+ assignment appears the only thing possible, but the 2+, 3 level, predicted at 1.75 Mev, should decay about 90% to the 2+, 1 level, and about 4% to the ground state. For the ground state transition, however, the cancellation factor C is very small (Table X), so that a small change in the wave functions could produce a large increase in the predicted transition rate to the ground state.

Comparison of Gamma Transition Rates with Experiment

Experimental relative gamma transition rates are shown in the last column of Table X, separately normalized for each parent level to unity for the strongest branch. The absolute rate of the 2+, $1\rightarrow 0$+, 1 decay is also indicated. It is significant and fortunate that this decay rate is not sensitive to small changes in the eigenfunctions, since it is used to adjust the neutron effective charge used to calculate other $E2$ rates. For this transition, every component of the transition amplitude has the same sign ($C=1.00$) and the rate is enhanced by about a factor two over that for pure states—just sufficient to make the collective coupling strength in Pb^{206} equal to that in Pb^{207}. Corresponding to the enhancement of the $E2$ transition from the lowest 2+ state are inhibitions of $E2$ transitions from the higher 2+ states. For example, the 2+, $2\rightarrow 0$+, 1 decay is inhibited relative to a pure state transition by a factor of more than 1000. As discussed earlier, the predicted rate is therefore completely unreliable, and the great discrepancy between theory and experiment for this transition is not very serious.

Among the many relative transition rates measured by Alburger,[4] those from four parent states—4+, 1; 4+, 2; 5−, 2; and 7−, 1—can be compared with theory. The predicted intensity ratio 4+, $1\rightarrow 2$+, 1: 4+, $1\rightarrow 3$+, 1 is 1:0.68. The experimental value is slightly uncertain because each of these two transitions may be masking weaker transitions of nearly the same energy (see Table V). For $\chi_1=\chi_2=0$, the experimental ratio is 1:0.38. For the rough guesses $\chi_1\approx 0.2$, $\chi_2\approx 0.007$ (based on total intensity consistency, see Table VI), the experimental ratio is 1:0.37.

The predicted intensity ratios 4+, $2\rightarrow 2$+, 1: 4+, $2\rightarrow 3$+, 1:4+, $2\rightarrow 4$+, 1 are 0.065:1:0.26, to be compared with the experimental ratios ~ 0:1:0.24. The $E2$ transition 4+, $2\rightarrow 2$+, 1 should indeed not have been seen, since it is a branch of a weakly populated parent, and has a very small conversion coefficient. The predicted intensity ratios from the 5−, 2 state are in good qualitative agreement with experiment (Table X), but there is a discrepancy factor of 5 in one ratio.

A good test of mixing in the two 4+ states is the relative rates 7−, $1\rightarrow 4$+, 1:7−, $1\rightarrow 4$+, 2, since the two transitions are predicted to take place from only a single component in the initial state, $(p_{1/2}i_{13/2})$, to the same single component in both final states, $(p_{1/2}f_{7/2})$. Here the intensity ratio depends only on the ratio of the amplitude of $(p_{1/2}f_{7/2})$ in the two final states, and is independent of the transition matrix element, and of the 7−, 1 eigenfunction. The predicted ratio is 1: 0.00056. The observed ratio is 1:0.00123, different by a factor two. This suggests that the theoretical eigenfunctions of the lowest 4+ states are not very good. There are, however, uncertainties in the observed intensity ratio which make it impossible to draw a definite conclusion from the comparison. The measured K-electron intensities contain some experimental error. In addition, the K-conversion coefficients introduce uncertainty, especially since they are quite different for the two transitions. Taken seriously, the observed ratio implies that the amplitudes of $(p_{1/2}f_{7/2})$ in the two 4+ states are nearly equal.

Table X suggests that there should be observable gamma rays which have not yet been seen following inelastic neutron scattering from Pb^{206}. Also one transition with measurable lifetime is predicted. A 0+ state is predicted at 1.23 Mev which decays with a 0.43-Mev gamma ray at a rate 3.15×10^8 sec^{-1}. After correction for conversion, this corresponds to a half-life for the state, $\tau_{1/2}=2.1\times 10^{-9}$ sec.

2. $Pb^{206}(d,p)Pb^{207}$ *Cross Sections*

If the (d,p) reaction proceeds predominantly by a direct stripping process, the parent and daughter states must differ only in the quantum numbers of one neutron. In the reaction $Pb^{206}(d,p)$ the low states of the daughter Pb^{207} are of an especially simple type, being described

as single neutron holes. Therefore the (d,p) cross section to a final state $(lj)^{-1}$ in Pb^{207} is a measure of the amplitude of $(lj)^{-2}$ in the ground-state wave function of Pb^{206}. The observed cross sections are in qualitative accord with theory. Transitions to the $f_{5/2}$ and $p_{3/2}$ levels in Pb^{207} are weaker than the transition to the $p_{1/2}$ level, and transitions to the $i_{13/2}$ and $f_{7/2}$ levels are not seen at all (see Table VII).

Quantitative comparison with theory can be made only for the ratios of the cross sections to the two p levels, because absolute magnitudes of theoretical (d,p) cross sections and ratios of cross sections for different l-values are in poor accord with experiment. But for the ratio $\sigma(p_{3/2})/\sigma(p_{1/2})$, the uncertain factors cancel. (We ignore also energy-dependent factors, since the energy of the incident deuterons is large compared to the $p_{3/2}-p_{1/2}$ energy difference.) One then has the simple theoretical result,[10]

$$\sigma(p_{3/2})/\sigma(p_{1/2})=2(a_{3/2})^2/(a_{1/2})^2, \tag{25}$$

where $a_{3/2}$ and $a_{1/2}$ are amplitudes of the $(p_{3/2})^2$ and $(p_{1/2})^2$ configurations in the ground state of Pb^{206}. The factor 2 is a statistical factor arising from the different final state spins of the transitions being compared. The theoretical value of $(a_{3/2}/a_{1/2})$ is 0.435. The empirical value of the same ratio is 0.375, found by substituting peak cross sections from Table VII on the left of (25). This comparison suggests that the actual mixing in the ground state is somewhat smaller than the calculated mixing. If one uses in (25) total cross sections instead of peak cross sections, the result is $(a_{3/2}/a_{1/2})_{\text{exp}}=0.392$. The ratio of peak cross sections seems more meaningful, however, since the stripping mechanism is presumably dominant at the peak. It will be observed in Table VII that the two peaks occur at nearly the same angle.

McEllistrem *et al.*[11] have pointed out that the additional knowledge of the $Pb^{207}(d,p)Pb^{208}$ cross section (ground-state transition) provides a means of determining the amplitudes $a_{1/2}$ and $a_{3/2}$ separately, in addition to their ratio. The Pb^{207} ground state is regarded as pure $p_{1/2}$, and the Pb^{208} ground state as pure $(p_{1/2})^2$. Since the neutron separation energies from Pb^{207} and Pb^{208} are not very different (see part VI), the energy dependent factors in the $Pb^{206}(d,p)$ and $Pb^{207}(d,p)$ reactions (to the states of interest) may be taken to be equal. Hence for the ground-state transitions, a formula as simple as (25) results[10]:

$$\sigma[Pb^{206}(d,p)]/\sigma[Pb^{207}(d,p)]=2(a_{1/2})^2. \tag{26}$$

McEllistrem *et al.*[11] find a peak cross section in the $Pb^{207}(d,p)$ experiment of 0.187 mb/steradian at 65° (see Table VII). From their experimental data, therefore, one finds $|a_{1/2}|=0.91$, $|a_{3/2}|=0.34$. The theoretical values (Table VIII) are $a_{1/2}=0.865$, $a_{3/2}=0.377$. A rough check on the experimentally derived amplitudes is provided by the fact that the sum of the squares of the two amplitudes have a reasonable value, 0.94. One would infer from this figure that the amplitude of $(f_{5/2})^2$ is about 0.23, to be compared with the theoretical value, 0.308. McEllistrem *et al.*[11] estimate the uncertainty in their cross-section measurements to be about $\pm 20\%$.

C. Remarks on Pb^{204}

In a highly simplified theory of Pb^{204}, similar to the theory of Alburger and Pryce[4] for Pb^{206} and utilizing the same parameters,[2] the lowest two 4+ states, arising from the configurations $(p_{1/2})_0^2 p_{3/2}f_{5/2}$ and $(p_{1/2})_0^2(f_{5/2})^2$, were predicted to be nearly degenerate and to be at an excitation energy of about 1.08 Mev.

In a more correct theory including configuration mixing, this excitation energy would undoubtedly be increased, due to an extra depression of the ground state. The pair of 4+ levels observed by Herrlander *et al.* (Table IV) lie at 1.274 Mev and 1.563 Mev (center of mass at 1.419).

A theoretical lower limit to the splitting of two near-degenerate levels is twice the magnitude of the matrix element of the energy connecting them. The matrix element connecting these two 4+ states is equal to the two-particle element, $\langle(f_{5/2})^2 4|V|p_{3/2}f_{5/2}4\rangle$, which, from our work on Pb^{206}, was calculated to be—0.106 Mev. We therefore can predict in Pb^{204}

$$(\Delta E)_{4+}>0.212 \text{ Mev}. \tag{27}$$

For levels which in first order are nearly degenerate, the splitting would be only slightly greater than this lower limit. The observed splitting is 0.289 Mev, in fair agreement with theory.

V. EFFECTS OF TRIPLET FORCES AND OF COLLECTIVE MOTION

A. Triplet Forces

The analysis of Gammel, Christian, and Thaler[14] gives for the potentials effective between identical nucleons an infinite repulsive core of radius $r_c=0.4\times10^{-13}$ cm, and Yukawa potentials beyond r_c:

$$\begin{aligned}&\text{Singlet-even,}\quad V=-425 \text{ Mev } \exp(0.69r)/(0.69r);\\ &\text{Triplet-odd,}\quad V=-\ 14 \text{ Mev } \exp(r)/r;\\ &\text{Tensor-odd,}\quad V=+\ 22 \text{ Mev } \exp(0.8r)/(0.8r).\end{aligned} \tag{28}$$

Distances are measured in units of 10^{-13} cm. The triplet-odd force is attractive and much weaker than the singlet-even. The tensor force is attractive for the $^3P_0$ state and somewhat stronger than the triplet-odd, but still weak compared to the singlet-even. We have therefore ignored the odd-state forces in our detailed calculation. The effective force in the shell model need not have the same exchange character as the free two-body force, but in the absence of any contrary evidence, we continue to assume that it has.

We have done a crude calculation to test the effect of some triplet force on our results. The triplet potential was taken to have the same shape (Gaussian) and range as the singlet potential, to be one third as strong

as the singlet potential, and to be either attractive or repulsive. It was included in the diagonal elements only for spins 0 through 4 and the energy levels were recalculated for these spin values. The results were changed only slightly, and the agreement with experimental energy levels was still good for both attractive and repulsive triplet forces (see Table XI). The eigenfunctions were also not greatly altered. Somewhat greater alteration of the eigenfunctions would be expected for a better calculation including the off-diagonal triplet matrix elements. Comparison with Kearsley's results[6] (next section) gives more insight into the role of the triplet forces.

The reason the weak triplet force changes the results so little is that it produces a similar shift on all the levels and smaller relative shift. For our choice of triplet strength$=\frac{1}{3}$ (singlet strength), the relative shifts produced by the triplet force are at most about one-sixth of the relative shifts produced by the singlet force.

TABLE XI. Effect of weak triplet forces.

Spin and parity	Theoretical energies: Pure singlet	Singlet plus $\frac{1}{3}$ (Attractive triplet)	Singlet plus $\frac{1}{3}$ (Repulsive triplet)	Experimental energies
0+	0.01[a]	0.02	0.04	0
1+	1.71	1.67	1.72	1.73
2+	0.81	0.84	0.75	0.803
2+	1.26	1.30	1.19	1.46
3+	1.34[a]	1.34[a]	1.34[a]	1.341
4+	1.71	1.75	1.66	1.684
4+	1.97	2.01	1.92	1.998
Configuration	Eigenfunction of lowest 2+ state			
$p_{1/2}f_{5/2}$	0.723	0.737	0.700	
$p_{1/2}p_{3/2}$	−0.602	−0.581	−0.660	
$(f_{5/2})^2$	0.217	0.221	0.214	
$p_{3/2}f_{5/2}$	0.151	0.156	0.149	
$(p_{3/2})^2$	0.213	0.214	0.227	

[a] Energies normalized to 3+ level.

B. Comparison with Kearsley Results

The parameters of Kearsley's calculation are compared with ours in Table XII. Since there are a number of points of difference, it is interesting to observe the similarity in the results. Kearsley's nuclear size is 18% larger than ours. She uses a Yukawa potential and we a Gaussian. These potentials are probably best compared through the singlet-even effective range and strength parameter, s (see reference a, Table XII). Her effective range is 7.5% smaller than ours, and her singlet strength parameter, s, 11% larger than ours. Aside from the shapes of the potentials, the only large difference in the two sets of parameters is in the exchange mixture. Her triplet-odd force is taken to be repulsive and more than half as great in magnitude as the singlet-even force, while our triplet-odd force is zero. (The singlet-odd and triplet-even parts of the "Rosenfeld-mixture"[33] force which she uses of course play no role in this calculation.)

[33] L. Rosenfeld, *Nuclear Forces* (North-Holland Publishing Company, Amsterdam, 1948), p. 234.

TABLE XII. Comparison of Kearsley parameters and parameters used in this paper.[a]

Quantity	Kearsley[b]	This paper
Two-body potential shape	Yukawa	Gaussian
Range parameter of potential (10^{-13} cm)	1.37	1.85
Depth parameter of singlet potential	42 Mev	32.5 Mev
Singlet: triplet ratio	−1: +0.559	−1: 0
Singlet effective range, r_{0s} (10^{-13} cm)	2.45	2.65
Singlet strength parameter, s[c]	1.11	1.00
Wave functions	Harmonic oscillator	Harmonic oscillator
Nuclear size parameter, b[d] (10^{-13} cm)	2.70	2.33

[a] In this table, "singlet" refers only to singlet-even, and "triplet" only to triplet-odd.
[b] See reference 6.
[c] The strength parameter s is defined in J. M. Blatt and V. F. Weisskopf, *Theoretical Nuclear Physics* (John Wiley and Sons, Inc., New York, 1952), p. 55. For $s=1.00$, there is a ^1S bound state at zero energy. For $s>1$, there is a ^1S bound state below zero.
[d] The size parameter b is defined by Eq. (4).

It seems significant that the singlet forces in the two calculations are nearly equal in strength. This confirms the result of the previous section that the triplet forces produce smaller relative shifts in level positions than do the singlet forces. Therefore the effect of triplet forces on the calculated level spectrum is considerably smaller than one might infer by examining the relative magnitudes of singlet and triplet matrix elements for a given spin and parity.

Sample comparisons of our results with those of Kearsley are shown in Table XIII. It is remarkable that the two sets of theoretical results agree so very closely, even in the eigenfunctions. For the energy of the second 2+ state, for example, the two theories agree with each

TABLE XIII. Comparison of some Kearsley results with results in this paper.

A. Some energy levels[a] (in Mev)

Spin and parity	Kearsley	This paper	Experiment
0+	0	0	0
1+	1.70	1.70	1.73
1+	2.32	2.27	(2.15)
2+	0.87	0.80	0.803
2+	1.22	1.24	1.46
3+	1.31	1.33	1.341
4+	1.69	1.70	1.684
4+	1.94	1.95	1.998
5−	2.88	2.88	2.783
6−	2.37	2.42	2.385
7−	2.19	2.21	2.200

B. Ground-state eigenfunction

	$(p_{1/2})^2$	$(f_{5/2})^2$	$(p_{3/2})^2$	$(i_{13/2})^2$	$(f_{7/2})^2$
Kearsley	0.840	0.332	0.379	−0.139	0.142
This paper	0.865	0.308	0.377	−0.122	···

C. Lowest 2+ eigenfunction[b]

	$(p_{1/2}f_{5/2})$	$(p_{1/2}p_{3/2})$	$(f_{5/2})^2$	$(p_{3/2}f_{5/2})$	$(p_{3/2})^2$	$(p_{3/2}f_{7/2})$
Kearsley	0.766	−0.530	0.233	−0.123	0.182	0.135
This paper	0.723	−0.602	0.217	0.151	0.213	···

[a] For this comparison, we have normalized our levels to the ground state.
[b] Kearsley also includes three other configurations in this eigenfunction. Each has an amplitude less than 0.07.

other much more closely than either agrees with experiment. In the diagonalization process, Kearsley included more levels than we, but the extra levels all have small amplitudes, and the larger calculated amplitudes for states included in both calculations are in rather close agreement. The eigenfunctions of the lowest 0+ state and lowest 2+ state, both of which have large mixing, are compared in Table XIII. The only apparent discrepancy is in the amplitudes of the $(p_{3/2}f_{5/2})$ state, which are small but have opposite sign in the two calculations.[34]

From comparisons of these two calculations, one may conclude that the results are quite insensitive to the shape of the two-body potential and to the exchange mixture. (The latter conclusion might not hold for calculations involving the neutron-proton force, where all four exchange possibilities enter.) Kearsley has shown that the results do depend rather sensitively on the strength of the potential. Comparison with our results suggests that the sensitivity is mainly to the singlet part of the potential, which in her calculation turns out to have, and in our calculation is assumed to have, nearly the same strength as the singlet-even potential observed in the two-nucleon system. The ratio of the effective range of the two-body force, r_{0s}, to the nuclear size parameter, b, is 0.91 in Kearsley's calculation and 1.14 in ours. This difference appears to have no marked effect on the results.

C. Weak Coupling to Collective Motion

The wave functions which have been assumed so far for the neutron-hole states in Pb^{206} would imply that no electric quadrupole radiation occurs between the states. We shall assume that such radiation arises from ellipsoidal vibrations of the nuclear core, weakly coupled to the particle motion. We use the collective Hamiltonian of Bohr and Mottelson,[28] assigning extra degrees of freedom to the core vibration, and use the weak-coupling (one phonon) formalism.[35–37] From the observed rate of the $E2$ transition between the first excited state and ground state in Pb^{206}, one may deduce a strength of particle-core coupling—or, approximately, a nuclear surface tension. This coupling strength may then be used to calculate other $E2$ transition rates in Pb. Finally, for internal consistency, one must use the same coupling strength to estimate the effect of the collective motion on the positions of the energy levels.

1. Effective Charge Concept for Neutron Transitions

We consider first states, $|\Gamma I\rangle$, of neutrons only, which are some arbitrary superposition of pure shell-model states, $|\beta I\rangle$, where β represents the quantum numbers of a pure configuration, e.g., in the j-j coupling representation:

$$|\Gamma I\rangle=\sum_\beta a_\beta|\beta I\rangle. \tag{29}$$

Now let a weak coupling to collective motion act as a perturbation on this state. The states of the coupled system we denote by $|\beta''J'';NR;I\rangle$, representing the vector coupling of a particle state $\beta''J''$ to a collective state of N phonons and angular momentum R to yield total angular momentum I. In the one-phonon approximation, in which the phonon energy, $\hbar\omega$, is assumed to be large compared to the spacings of the particle levels, the state $|\Gamma I\rangle$ becomes[37]

$$|\Gamma I\rangle=\sum_\beta a_\beta\{|\beta I;00;I\rangle+(2I+1)^{-\frac{1}{2}}\sum_i\sum_{\beta''J''}\langle\beta|\xi_i|\beta''\rangle \times\langle\beta I\|\mathcal{Y}_2(i)\|\beta''J''\rangle|\beta''J'';12;I\rangle\}. \tag{30}$$

The amplitudes of the admixed one-phonon states have been entered explicitly. $\mathcal{Y}_{2\mu}(i)$ is equal to $(\pi/5)^{\frac{1}{2}}\times Y_{2\mu}(\theta_i\varphi_i)$, where i labels the particles, and its reduced matrix element is understood to be taken between the angular parts of the particle wave functions only. The quantity ξ_i is equal to $k(r_i)\gamma/\hbar\omega$ and its matrix element is understood to be taken between the radial parts of the particle wave functions only. The function $k(r_i)$ is taken usually to be proportional to $\delta(r_i-R)$; and $\gamma=(5\hbar\omega/2\pi C)^{\frac{1}{2}}$, where C is the surface tension parameter.[28] The radial matrix element, $\langle\beta|\xi_i|\beta''\rangle$, has usually been assumed to be approximately constant, and has been called simply ξ and taken outside the sum. An important thing to notice, however, is that the sign of ξ may be either positive or negative, according to the relative signs of the radial wave functions near the nuclear surface. Bohr and Mottelson have pointed out[28] that ξ should have opposite signs for particles and for holes, but its sign may also change according to the convention adopted for the signs of the radial wave functions. In a calculation like the present one, in which mixed states are considered, such sign questions are very important.

The reduced transition probability, $B_e(2)$, for electric quadrupole radiation from initial state $|\Gamma'I'\rangle$ to final state $|\Gamma I\rangle$ is

$$B_e(2)=(2I'+1)^{-1}|\langle\Gamma I\|Q_2\|\Gamma'I'\rangle|^2. \tag{31}$$

The collective quadrupole operator is[28,37]

$$Q_{2m}{}^c=\tfrac{1}{4}(5\pi)^{-\frac{1}{2}}3ZeR^2\gamma[b_m+(-1)^m b_{-m}{}^*], \tag{32}$$

where b_m is a phonon annihilation operator. This operator connects only states with the same particle configuration which differ by one phonon. Making use of the expansion (30), and taking advantage of the tensor properties[24] of the operator (32), one finds for the reduced matrix element of $Q_2{}^c$ needed in (31),

$$\langle\Gamma I\|Q_2{}^c\|\Gamma'I'\rangle=(3ZeR^2/4\pi)(1/C) \times\sum_i\sum_{\beta,\gamma}\langle\beta|k_i|\gamma\rangle a_\beta{}^* a_\gamma{}'\langle\beta I\|\mathcal{Y}_2(i)\|\gamma I'\rangle. \tag{33}$$

[34] The signs of the amplitudes of the $(p_{1/2}p_{3/2})_2$ state and the $(p_{3/2}f_{5/2})_2$ state are opposite in Table XIII to those in Kearsley's paper, because she writes the two-particle state differently, as $(p_{3/2}p_{1/2})_2$ and $(f_{5/2}p_{3/2})_2$. For two-particle antisymmetrized functions, $|jj'I\rangle=(-1)^{j+j'+I+1}|j'jI\rangle$.

[35] D. C. Choudhury, Kgl. Danske Videnskab. Selskab, Mat.-fys. Medd. **28**, No. 4 (1954).

[36] A. Kerman, Phys. Rev. **92**, 1176 (1953).

[37] K. Ford and C. Levinson, Phys. Rev. **100**, 1 (1955).

Now for protons, the quadrupole operator is

$$Q_{2m}{}^{p}=e\sum_i r_i{}^2Y_{2m}(i). \tag{34}$$

We see that the reduced matrix element (33) for the collective transition between neutron states is the same as one would obtain by ignoring the collective motion and utilizing for the neutrons a quadrupole particle operator of a form similar to that for protons,

$$Q_{2m}{}^{n}=(3ZeR^2/4\pi C)\sum_i k(r_i)Y_{2\mu}(i). \tag{35}$$

Because the states are antisymmetrized, the sum over the particle label i on the right of (32) may be replaced by a factor n (for n particles) with i set equal to 1 (or to any other particular particle label). Therefore comparison of (34) and (35) shows that the collective transition rate for neutron states differs from the particle transition rate for the same proton states only by the square of a factor which we may define to be the (neutron effective charge/proton charge). This factor is given by

$$(e_{\text{eff}}/e)=(3Z/4\pi C)(\langle k\rangle R^2/\langle r^2\rangle), \tag{36}$$

where $\langle k\rangle$ indicates the matrix element of $k(r_1)$ between initial and final states, and $\langle r^2\rangle$ the matrix element of $r_1{}^2$ between the same two states. These matrix elements are expected to be generally of the same order of magnitude for all states in a given nucleus, so that the effective neutron charge will be nearly the same for all $E2$ transitions in a given nucleus. For example, we may set $\langle k\rangle\cong\pm k$, where k is a positive constant (≈ 40 Mev), and $\langle r^2\rangle\cong\pm\frac{3}{5}R^2$. The plus (minus) sign is taken if the radial wave functions have the same (opposite) sign near the nuclear surface. With this approximation,

$$(e_{\text{eff}/e})\cong(5Z/4\pi)(k/C). \tag{37}$$

This is the approximate form which we use in Pb^{206}. Explicit calculation with harmonic oscillator functions shows that $\langle r^2\rangle$ is indeed nearly constant in magnitude for all of the states of interest in Pb^{206} (Table XIV). We assume that the matrix elements of $k(r)$ are likewise nearly constant in magnitude and have the same sign as the matrix elements of r^2 (negative for any matrix element involving an odd number of f states, otherwise positive). In the actual calculations of transition rates, we used the approximate effective charge (37), and set all matrix elements of $\langle r^2\rangle$ equal to $\pm\frac{3}{5}(1.20A^{\frac{1}{3}})^2$ $=\pm 30.1(10^{-13}\text{ cm})^2$.

If the states weakly coupled to collective motion are proton states instead of neutron states, the quadrupole operator is the sum of the operators (32) and (34). These produce simply additive effects in the matrix elements, so that the effective charge for proton transition is obtained by adding unity to the right side of Eq. (36) or (37).

TABLE XIV. Matrix elements of r^2 for one-particle states relevant in Pb^{206}. Distance units are 10^{-13} cm.

$\langle p\|r^2\|p\rangle=$	35.3 =	$\frac{3}{5}(1.30A^{\frac{1}{3}})^2$
$\langle f\|r^2\|f\rangle=$	35.3 =	$\frac{3}{5}(1.30A^{\frac{1}{3}})^2$
$\langle i\|r^2\|i\rangle=$	40.7 =	$\frac{3}{5}(1.39A^{\frac{1}{3}})^2$
$\langle p\|r^2\|f\rangle=$	-32.6 =	$-\frac{3}{5}(1.25A^{\frac{1}{3}})^2$

2. *Strength of Collective Motion in* Pb^{206} *and Effective Charge of Neutron*

In an earlier paper,[2] the known electric quadrupole transition rates between the lowest two states in both Pb^{207} and Pb^{206} (Sec. II) were used to evaluate the strength of collective motion in these nuclei. If, for Pb^{207}, one takes $R=1.20A^{\frac{1}{3}}\times 10^{-13}$ cm, and assumes the states to be pure single neutron hole states weakly coupled to collective motion, one obtains $(k/C)=0.0345$. If k is taken to be 40 Mev, this figure gives for the surface tension, $C=1160$ Mev. The neutron effective charge is $e_{\text{eff}}=1.13e$. The uncertainty in the measured transition rate is about 25%. Hence the uncertainty in the derived values of (k/C) and of e_{eff} is about 12%.

In the previous work[2] for Pb^{206}, an error of a factor $\sqrt{2}$ was made in the electric quadrupole matrix element. The result given there should have been (for $k=40$ Mev), $C=780$ Mev instead of $C=550$ Mev. Pure states were assumed in that calculation, $(p_{1/2}f_{5/2})_2\rightarrow(p_{1/2})_0{}^2$. We have re-evaluated this transition rate from the first excited state to the ground state in Pb^{206}, using the calculated eigenfunctions in Table VIII. The result of the mixing is to enhance the transition rate, thus diminishing the strength of collective coupling required to give the observed rate. The result for the coupling strength is $(k/C)=0.0351$, implying an effective neutron charge, $e_{\text{eff}}=1.15e$, in excellent agreement with the results in Pb^{207}. The uncertainty in these numbers is also about 12%. If k is set equal to 40 Mev, one finds, for Pb^{206}, $C=1140$ Mev. All $E2$ transition rates in Pb^{206} have been calculated using $e_{\text{eff}}=1.15e$, and $R=1.20A^{\frac{1}{3}}\times 10^{-13}$ cm.

It is interesting that the calculated mixing is just sufficient to remove the discrepancy in the calculated collective coupling strengths in Pb^{206} and Pb^{207}. The signs of the mixture amplitudes for the lowest 2+ state and the lowest 0+ state are such that all eight components of the transition matrix element add together with the same sign, and the net transition rate is twice as great as between the pure configurations $(p_{1/2}f_{5/2})$ and $(p_{1/2})^2$. At the same time this means that the calculated rate is not very sensitive to the exact degree of mixing. The $E2$ transition rates from the higher 2+ states to the ground state are inhibited relative to pure state transitions and are therefore more sensitive to the calculated degree of mixing (see Table X). The numbers given above are summarized in Table XV.

In Pb^{204} the measured transition rate from the lowest 4+ state to the lowest 2+ state is anomalously slow. A highly simplified shell model calculation[2] has shown that large mixing is expected for the states. It will be interesting to learn whether a detailed theory of this

TABLE XV. Collective parameters in Pb^{206} and Pb^{207}.

Nucleus	$(k/C)^a$	Assumed k	C	e_{eff}/e^a	(k^2/C)
Pb^{206}	0.0351	40 Mev	1140 Mev	1.15	1.4 Mev
Pb^{207}	0.0341	40 Mev	1160 Mev	1.13	1.4 Mev

[a] Uncertainty from experiment, ±12%.

mixing will lead to cancelling transition matrix elements, which may explain the slow rate of the transition.

3. *Effect of Collective Motion on Energies*

In the weak-coupling, one-phonon, approximation, the effect of collective motion on the energy levels may be found by adding to the direct interaction among the extra nucleons an effective two-body potential,

$$V_{12}=-(\pm k^2/C)(5/4\pi)P_2(\cos\theta_{12}), \qquad (38)$$

where P_2 is a Legendre polynomial and θ_{12} is the angle between the radius vectors to particles 1 and 2. The radial part of the matrix element is assumed to be evaluated already and to lead to the same magnitude of k^2 for all states. For a matrix element between state i and state j, the factor $\pm k^2$ represents the product $\langle i|k(r)|m\rangle\langle m|k(r)|j\rangle$, or a sum of such products, where m represents an intermediate state. The sign preceding k^2 therefore depends on the signs of the radial wave functions near the nuclear radius in states i and j. For the states of interest in Pb^{206}, the negative sign applies when states i and j contain together an odd number of f particles; otherwise the positive sign applies.

In order to evaluate matrix elements of the effective potential (38), it is more convenient to write it in expanded form,

$$V_{12}=-(\pm k^2/C)\sum_\mu Y_{2\mu}(\theta_1\varphi_1)Y_{2\mu}{}^*(\theta_2\varphi_2), \qquad (39)$$

which, by the definition of Racah,[24] is the scalar product of two second rank tensors. Racah's method may be used to evaluate the matrix elements of (39). We are here interested only in the matrix elements between two-particle states.

Case A, $j_1\neq j_2$, $j_1'\neq j_2'$:

$$\langle j_1j_2J|V_{12}|j_1'j_2'J\rangle=(\pm k^2/C)(-1)^{j_1+j_2'+1}$$
$$\times[(-1)^J\langle j_1\|Y_2\|j_1'\rangle\langle j_2\|Y_2\|j_2'\rangle W(j_1j_1'j_2j_2';2J)$$
$$+\langle j_1\|Y_2\|j_2'\rangle\langle j_2\|Y_2\|j_1'\rangle W(j_1j_2'j_2j_1';2J)]. \qquad (40)$$

For Case B, $j_1=j_2$, $j_1'\neq j_2'$, (40) should be multiplied by $2^{-\frac{1}{2}}$. For Case C, $j_1=j_2$, $j_1'=j_2'$, (40) should be multiplied by $\frac{1}{2}$ [or equivalently, the first term in (39) retained and the second term dropped].

The measured $E2$ transition rate in Pb^{206} leads to a value $k/C=0.035$ for the ratio of the collective model parameters k and C. The energy shifts for weak coupling are also independent of the mass parameter B, but depend on a different combination of k and C, namely, k^2/C. We must therefore assume a value of k (or C) in order to evaluate the energy shifts. We choose $k=40$ Mev, which implies $k^2/C=1.4$ Mev. For this value of k^2/C, the matrix elements (40) were evaluated for the states of interest in Pb^{206}—both diagonal and off-diagonal. These were added to the previously determined singlet matrix elements, and the energies re-evaluated, the same number of states being diagonalized for each spin value as with singlet forces alone.[38]

The energy level results with the full strength of singlet forces, plus collective coupling, are much less satisfactory than with pure singlet forces. The sensitivity of the energy results to a small degree of collective motion comes about because the effective force from collective coupling is repulsive for some states and attractive for others. In particular it is attractive for the lowest 0+ and 2+ states but repulsive for the lowest 3+ state. Therefore the pattern is easily distorted.

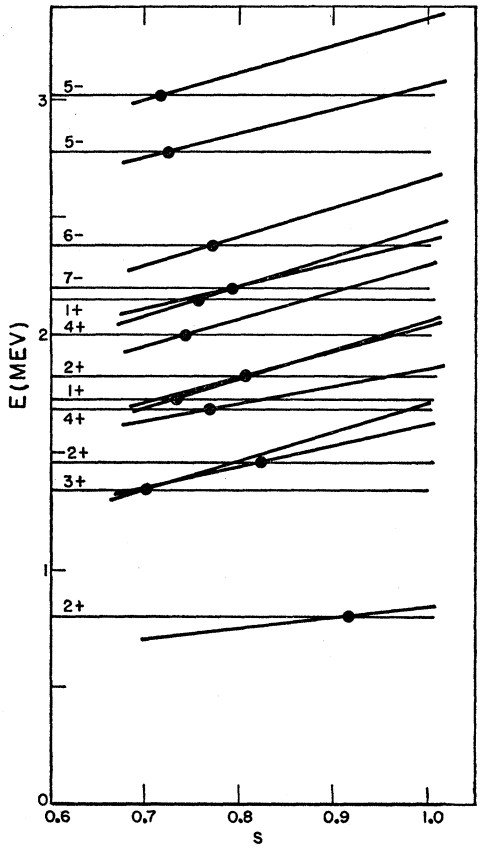

FIG. 4. Calculated energies as a function of the singlet strength parameter, s, for fixed strength of collective coupling, characterized by $k^2/C=1.4$ Mev. Light horizontal lines are empirical levels. The dots mark the intersection of corresponding empirical and theoretical level positions.

[38] Collective matrix elements were evaluated, and matrices diagonalized, on an IBM 704 computer at the Los Alamos Scientific Laboratory. We are indebted to S. Blumberg and T. Jordan for help with the numerical work.

Nevertheless good agreement with experimental energy levels can again be obtained with this degree of collective motion ($k^2/C=1.4$ Mev) if the strength of the singlet force is diminished to about 75% of its previous value. We adopted a potential, s(singlet) +(collective), and diagonalized the energy matrices for several values of s between 0.7 and 1.0 ($s=1$ means the full strength of singlet force, s being the strength parameter defined in reference 27). The results, compared with experimentally known energy levels, are given in Fig. 4 as a function of s. The best over-all agreement with experiment occurs for $s\approx 0.75$.

4. *Results with 75% Singlet Forces Plus Collective Coupling*

We have regarded the strength of collective coupling as fixed by the observed $E2$ transition rate in Pb^{206}, and adjusted the strength parameter s of the singlet force to a value of 0.75 to give a good agreement with experimental energy levels. In Fig. 5 are compared the energy results for pure singlet forces ($s=1$), the results for $s=0.75$ with collective coupling (called hereafter singlet plus collective), and the experimental energies. The weaker singlet force with collective coupling gives improved overall energy agreement. In particular the predicted position of the 2+, 2 state is increased from 1.25 to 1.39 Mev, to be compared with the experimental value of 1.46 Mev. For the thirteen known levels, the mean deviation, $(13)^{-1}\sum|E_{\text{theory}}-E_{\text{exp}}|$, has the value 0.0572 Mev for pure singlet forces, and 0.0352 Mev for the singlet plus collective theory.

Theoretical energies and eigenfunctions for the singlet plus collective theory are given in Table XVI, to be compared with Table VIII. The mixing for the 6− levels is substantially greater in Table XVI. Otherwise

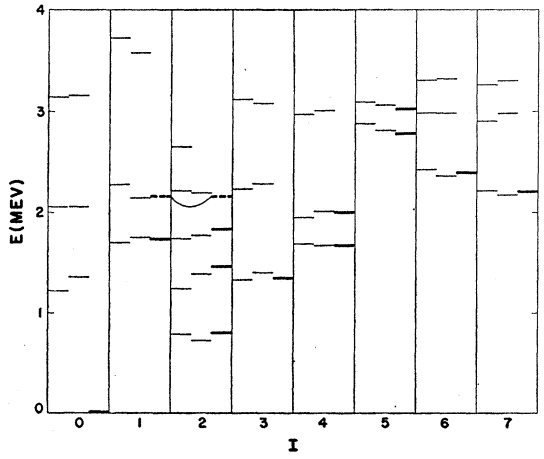

FIG. 5. Comparison of energies predicted with pure singlet forces (first column for each spin value), energies predicted with 75% singlet forces plus collective coupling (second column for each spin value), and empirical energies (third column for each spin value). Both sets of theoretical energies are normalized to the ground state.

TABLE XVI. Energy levels and eigenfunctions calculated for 75% singlet forces plus collective coupling ($k^2/C=1.40$ Mev) in Pb^{206}. Energies normalized to ground state.

Energy (Mev)	Eigenfunctions				
$I=0+$	$(p_{1/2})^2$	$(f_{5/2})^2$	$(p_{3/2})^2$	$(i_{13/2})^2$	
0	0.8548	0.3630	0.3589	−0.0933	
1.363	−0.4230	0.8944	0.0713	−0.1266	
2.056	−0.3002	−0.2238	0.9249	−0.0652	
3.162	−0.0064	0.1344	0.1042	0.9854	
$I=1+$	$(p_{1/2}p_{3/2})$	$(p_{3/2}f_{5/2})$		$(f_{5/2}f_{7/2})$	
1.745	0.9952	0		0.0977	
2.141	0	1.00		0	
3.576	−0.0977	0		0.9952	
$I=2+$	$(p_{1/2}f_{5/2})$	$(p_{1/2}p_{3/2})$	$(f_{5/2})^2$	$(p_{3/2}f_{5/2})$	$(p_{3/2})^2$
0.725	0.7526	−0.5456	0.2627	0.1663	0.1980
1.391	0.6105	0.7750	−0.0333	0.0206	−0.1585
1.767	−0.1629	0.1607	0.9564	−0.1692	−0.0656
2.190	−0.1774	0.1339	0.1228	0.9647	0.0705
2.527	−0.0524	0.2408	−0.0033	−0.1130	0.9625
3.494	$(p_{3/2}f_{7/2})$				
3.553	$(f_{5/2}f_{7/2})$				
$I=3+$	$(p_{1/2}f_{5/2})$	$(p_{3/2}f_{5/2})$		$(p_{1/2}f_{7/2})$	
1.404	0.9992	0.0361		−0.0150	
2.278	−0.0366	0.9988		−0.0325	
3.081	0.0138	0.0331		0.9994	
3.696	$(f_{5/2}f_{7/2})$				
3.985	$(p_{3/2}f_{7/2})$				
$I=4+$	$(f_{5/2})^2$		$(p_{3/2}f_{5/2})$	$(p_{1/2}f_{7/2})$	
1.675	0.6425		0.7157	−0.2740	
2.013	0.7631		−0.6304	0.1428	
3.010	0.0702		0.3010	0.9510	
3.592	$(f_{5/2}f_{7/2})$				
3.857	$(p_{3/2}f_{7/2})$				
$I=4-$					
2.845	$(f_{5/2}i_{13/2})$				
$I=5-$	$(f_{5/2}i_{13/2})$		$(p_{3/2}i_{13/2})$		
2.809	0.8137		−0.5812		
3.063	0.5812		0.8137		
$I=5+$					
3.733	$(f_{5/2}f_{7/2})$				
4.107	$(p_{3/2}f_{7/2})$				
$I=6-$	$(p_{1/2}i_{13/2})$		$(f_{5/2}i_{13/2})$	$(p_{3/2}i_{13/2})$	
2.355	0.9867		0.1447	0.0741	
2.982	−0.1317		0.9788	−0.1568	
3.321	−0.0951		0.1450	0.9849	
$I=6+$					
3.154	$(f_{5/2}f_{7/2})$				
$I=7-$	$(p_{1/2}i_{13/2})$		$(f_{5/2}i_{13/2})$	$(p_{3/2}i_{13/2})$	
2.166	0.9540		0.2490	−0.1671	
2.983	−0.2609		0.9639	−0.0535	
3.296	0.1477		0.0946	0.9845	
$I=8-$					
2.970	$(f_{5/2}i_{13/2})$				
3.236	$(p_{3/2}i_{13/2})$				
$I=9-$					
2.600	$(f_{5/2}i_{13/2})$				

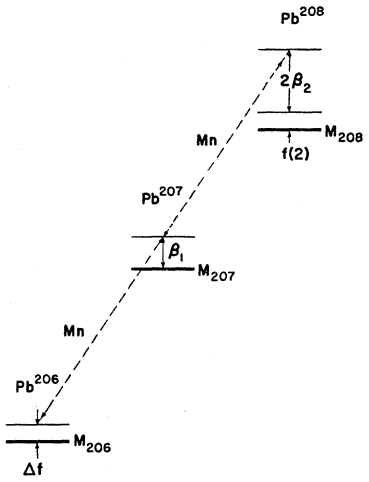

FIG. 6. Schematic representation of absolute energies. Notation is explained in the text.

the results are qualitatively similar. We regard these results as more reliable than the pure singlet results, because the effect of collective coupling on the energies must for self-consistency be included if its effect on transition rates is included. The absolute energy shift of the ground state from its zero-order position was 0.811 Mev for pure singlet forces, and is 0.751 Mev for singlet plus collective forces.

The eigenfunctions in Table XVI have been used to recalculate all $M1$ and $E2$ transition rates. The $2+$, $1\rightarrow 0+$, 1 transition rate, which was used to determine the strength of coupling, is altered by only 2%, so that no change in the coupling strength is required to preserve consistency. Because the cancellation factor C is equal to 1 for this transition, the predicted rate is not sensitive to small changes in the eigenfunctions. Other transition rates are altered by a greater amount. The predicted transition rates and comparison with experiment are presented in Table XVII, to be compared with Table X. The differences are, for most transitions, not great. Where comparison with experiment can be made, the predictions in Table XVII are about equally as good as those in Table X. One improvement is the $2+$, $2\rightarrow 0+$, 1 transition, which, although still strongly inhibited, is considerably changed in the direction toward agreement with experiment. The predicted decay from the $2+$, 3 level remains in disagreement with experiment. The branching ratio from the $7-$, 1 level to the two $4+$ levels is in somewhat poorer agreement with experiment.

VI. ABSOLUTE ENERGIES

In Fig. 3 and in Table VIII, the calculated energies have been normalized arbitrarily to agree with experiment for the lowest $3+$ level at 1.341 Mev, and in Fig. 5 and Table XVI, normalized to the ground state. However, the predicted absolute binding energy contribution of the interaction of the two holes in Pb^{206} may also be compared with experiment. We use a semiempirical mass formula for the core and take explicit account of the neutron holes.

Binding energy contributions are shown schematically in Fig. 6. The heavy line in the center labeled M_{207} represents the mass of Pb^{207}. We may think of forming Pb^{206} by removing one "valence" $p_{1/2}$ neutron from Pb^{207}. The mass change comes from several sources: (a) There is a mass increase of β_1, the binding energy of the $p_{1/2}$ neutron level in the average field of the other particles. (b) There is a mass decrease of M_n, the neutron mass. (c) There is a mass decrease of Δf, the energy lowering due to the possibility of virtual excitation of neutrons into the now empty $p_{1/2}$ level (i.e., configuration mixing). (d) There is an energy change of the core of 206 particles, due to its change of size (distinct from the shell model effect taken explicitly into account by Δf). The first three of these energies are indicated in Fig. 6.

Similarly, if one adds to Pb^{207} a neutron, there will be several contributions to the change of mass. (a) The binding energy of the $p_{1/2}$ level will be changed from β_1 to β_2, and the energy lowered by an amount $2\beta_2-\beta_1$. (b) There is a mass increase M_n. (c) There is a mass decrease $f(2)$, the interaction energy of the two $p_{1/2}$ neutrons (diagonal only, since, ignoring excitation to the next shell, configuration mixing is not possible). (d) There is an energy change of the core of 206 particles due to its change of size. Let us call this core energy $E_c(A)$, a function of mass number A.

The experimental separation energies will be,

$$E[206(n,\gamma)207]=\beta_1-\Delta f-E_c(207)+E_c(206).$$
$$E[207(n,\gamma)208]=2\beta_2-\beta_1+f(2)-E_c(208)+E_c(207). \quad (41)$$

Since we have no theory of the absolute position of the $p_{1/2}$ levels, it is necessary to take the difference of these separation energies. We approximate β and E_c as continuous smooth functions of A and write

$$E[207(n,\gamma)208]-E[206(n,\gamma)207]=\Delta^2B=f(2)+\Delta f+2(d\beta/dA)-(d^2E_c/dA^2). \quad (42)$$

We note that the discussion leading to (42) could have been in terms of holes instead of particles. In that case $f(2)$ and Δf would both have appeared as energy contributions in Pb^{206} and neither in Pb^{208}, but the result (42) would have been the same.

As a first approximation, one could assume that $\beta_1=\beta_2$ and that E_c is linear in A over the narrow range of A considered. Then the right side of (42) becomes the shell model energy $f(2)+\Delta f$. From our calculation with singlet forces, $f(2)=0.427$ Mev, $\Delta f=0.373$ Mev, $f(2)+\Delta f=0.800$ Mev. For singlet plus collective forces, $f(2)=0.321$ Mev, $\Delta f=0.430$ Mev, $f(2)+\Delta f=0.751$ Mev. Experimentally[12] (see Sec. II), the left side of (42) is equal to (0.65 ± 0.01) Mev, in fair agreement with $f(2)+\Delta f$. It is of some importance, however, to consider the correction terms, $2(d\beta/dA)-(d^2E_c/dA^2)$.

TABLE XVII. Gamma-ray transition rates in Pb^{206}, based on 75% singlet forces plus collective coupling.

Parent state	Energy (Mev)	Daughter state	Energy (Mev)	Transition energy (Mev)	Type	Rate (10^{12} sec^{-1})	Cancellation factor, C	Relative rate	Experiment
0+,2	(1.36)	2+,1	0.80	(0.56)	$E2$	0.00297	0.213	···	
0+,3	(2.15)	1+,1	1.73	(0.42)	$M1$	5.76	1.00	1	
		2+,1	0.80	(1.35)	$E2$	0.00140	0.0205	0.00024	
0+,4	(3.16)	1+,1	1.73	(1.43)	$M1$	1.10	0.734	1	
		1+,2	(2.15)	(1.01)	$M1$	~ 0	···	0	
		2+,1	0.80	(2.36)	$E2$	1.09	0.904	0.99	
1+,1	1.73	0+,1	0	1.73	$M1$	56.9	0.556	1	1
		0+,2	(1.36)	(0.37)	$M1$	0.212	0.706	0.0037	
		2+,1	0.80	0.93	$M1$	1.06	0.332	0.019	
		2+,2	1.46	0.27	$M1$	0.102	0.552	0.0018	
1+,2	(2.15)	0+,1	0	(2.15)	$M1$	~ 0	···	0	
		0+,2	(1.36)	(0.79)	$M1$	~ 0	···	0	
		1+,1	1.73	(0.42)	$M1$	~ 0	···	0	
		2+,1	0.80	(1.35)	$M1$	48.3	1.00	1	(1)
		2+,2	1.46	(0.69)	$M1$	2.76	1.00	0.057	
		3+,1	1.34	(0.81)	$E2$	0.0352	0.912	0.00073	
2+,1	0.803	0+,1	0	0.803	$E2$	0.105	1.00	···	$T=0.103\pm0.025$
2+,2	1.46	0+,1	0	1.46	$E2$	0.0102	0.0733	0.038	0.25
		2+,1	0.80	0.66	$M1$	0.271	0.235	1	1
2+,3	1.83	0+,1	0	1.83	$E2$	0.0176	0.114	0.0147	1
		2+,1	0.80	1.03	$M1$	1.20	0.456	1	
		2+,2	1.46	0.37	$M1$	4×10^{-8}	0.0006	~ 0	
		3+,1	1.34	0.49	$M1$	0.0048	0.328	0.0040	
2+,4	(2.15)	0+,1	0	(2.15)	$E2$	0.000815	0.0183	0.00005	
		1+,1	1.73	(0.42)	$M1$	0.0391	0.950	0.0026	
		2+,1	0.80	(1.35)	$M1$	15.0	0.569	1	(1)
		2+,2	1.46	(0.69)	$M1$	2.89	0.870	0.193	
		2+,3	1.83	(0.32)	$M1$	0.0089	0.315	0.00059	
		3+,1	1.34	(0.81)	$M1$	3.23	0.987	0.215	
3+,1	1.341	2+,1	0.803	0.538	$M1$	0.0280	0.355	···	
3+,2	(2.15)	2+,1	0.80	(1.35)	$M1$	4.63	0.428	0.68	
		2+,2	1.46	(0.69)	$M1$	0.876	0.790	0.128	
		2+,3	1.83	(0.32)	$M1$	0.00313	0.234	0.00046	
		3+,1	1.34	(0.81)	$M1$	6.84	0.995	1	
		4+,1	1.68	(0.47)	$M1$	0.931	0.947	0.136	
4+,1	1.684	2+,1	0.803	0.881	$E2$	0.172	0.939	1	$1-2.1x_2$
		3+,1	1.341	0.343	$M1$	0.124	0.368	0.72	$0.38-0.058x_1$
4+,2	1.998	2+,1	0.803	1.195	$E2$	0.0472	0.243	0.040	
		3+,1	1.341	0.657	$M1$	1.19	0.556	1	1
		4+,1	1.684	0.314	$M1$	0.307	1.00	0.26	0.24
5−,1	2.783	6−,1	2.385	0.398	$M1$	0.636	1.00	···	
5−,2	3.017	5−,1	2.783	0.234	$M1$	0.0541	0.796	0.0175	0.081
		6−,1	2.385	0.632	$M1$	3.09	0.845	1	1
		7−,1	2.200	0.817	$E2$	0.0147	0.464	0.0048	$0.075-30x_3$
6−,1	2.385	7−,1	2.200	0.185	$M1$	0.0189	0.563	···	
6−,2	(3.017)	5−,1	2.783	(0.229)	$M1$	0.0604	0.670	0.12	
		6−,1	2.385	(0.632)	$M1$	0.186	0.453	0.37	
		7−,1	2.200	(0.817)	$M1$	0.506	0.563	1	
7−,1	2.200	4+,1	1.684	0.5161	$E3$	···	···	1	1
		4+,2	1.998	0.2025	$E3$	···	···	0.00039	0.00123
7−,2	(2.98)	6−,1	2.385	(0.595)	$M1$	1.09×10^{-5}	0.0058	0.029	
		7−,1	2.20	(0.78)	$M1$	3.7×10^{-4}	0.0162	1	

Let $\beta=V-T$, where V is the potential well depth and T is the kinetic energy of the particle state of interest in the well. For small changes of radius R about some value R_0, T varies as R^{-2}. We suppose that the potential depth V varies as R^{-3}, i.e., as the density of core particles. Then,

$$\beta=-T_0(R_0/R)^2+V_0(R_0/R)^3. \quad (43)$$

The energy term needed in (42) is $2(d\beta/dA)$, which, evaluated at $R=R_0$ is

$$2(d\beta/dA)=2(-3V_0+2T_0)(R^{-1}dR/dA). \quad (44)$$

The last factor we write as

$$R^{-1}(dR/dA)=\gamma/3A. \quad (45)$$

The quantity γ would be unity for incompressible constant-density nuclei, and is less than unity for compressible nuclei (if Z is held constant and the change of A is due to change of neutron number). We adopt a value of 0.7 for γ, based on isotope-shift evidence about nuclear compressibility.[39,40] γ probably lies between 0.6 and 0.9.[40] Finally, we set $V_0=40$ Mev, $T=32$ Mev, and obtain the estimate,

$$2(d\beta/dA)\approx-0.13 \text{ Mev}. \quad (46)$$

For the core energy, E_c, we write

$$E_c=-\frac{3}{5}\frac{Z(Z-1)e^2}{R}-\alpha(A)A_0, \quad (47)$$

where A_0 is a constant, 126 in our case, and $\alpha(A)$ is taken to have the following form (volume energy plus surface energy):

$$\alpha(A)=\alpha_1[1+(1-R/R_0)]-\alpha_2(R_0/R)^2A^{-\frac{1}{3}}. \quad (48)$$

We shall not discuss the reasons for the particular R dependence of (48), since E_c turns out not to be important to our absolute energy calculation. (E_c itself is of course an extremely large energy, but its second derivative is small.) From a semiempirical mass formula,[16] we set $\alpha_1=15.6$ Mev, and $\alpha_2=(206)^{\frac{1}{3}}\times17.2$ Mev$=102$ Mev. A symmetry energy term has been left out of Eq. (47) because (47) represents the energy of a core of a fixed number of neutrons and protons. The symmetry energy effect is incorporated in the shell model energies, $f(2)$ and Δf. From (45), (47), and (48), one may evaluate the needed energy, (d^2E_c/dA^2). We find $d^2E_c/dA^2=-0.03$ Mev. The estimate for the total correction energy is then

$$2(d\beta/dA)-(d^2E_c/dA^2)\cong-0.10 \text{ Mev}. \quad (49)$$

The right side of (42) then has a theoretical value of 0.70 Mev for pure singlet forces or 0.65 Mev for singlet plus collective forces, which are to be compared with the experimental value of the left side, 0.65 Mev. The agreement is good, and suggests that mixing with higher neutron hole states does not depress the ground state of Pb^{206} very much. Indeed we found that the configuration $(i_{13/2})^2$ contributed only about -0.03 Mev to the ground-state energy, and $(f_{7/2})^2$ should contribute less than this amount.

In the above calculation it is important to get correctly only the effect of mixing which can occur in Pb^{206} and not in Pb^{207} or Pb^{208}. Admixtures of states of proton excitation, for example, should be similar in all three isotopes, and their effect on the energy difference calculated above should therefore be negligible. Hence we cannot conclude that the total energy shift produced by the sum of mixings to all higher states is negligible. We can conclude, however, that the magnitude of the calculated shell model energy, $f(2)+\Delta f$, is approximately correct.

VII. REMARKS ON EXPERIMENTS

A. $Pb^{207}(d,t)Pb^{206}$

The pick-up reaction $Pb^{207}(d,t)Pb^{206}$ is interesting because the one-particle selection rules should cause only states of the type $(p_{1/2}j)$ to be excited in Pb^{206}, and some of these—especially the 3+ and 4+ states of the $(p_{1/2}f_{7/2})$ configuration—are states which should not be easily excited by other means. The predicted levels which should be seen in this experiment are compared with the experimental results of Harvey (Table III, reference g) in Fig. 7. Within the limits of his poor energy resolution, the agreement with theory is good. He lists the level at 3.03 Mev as probably a

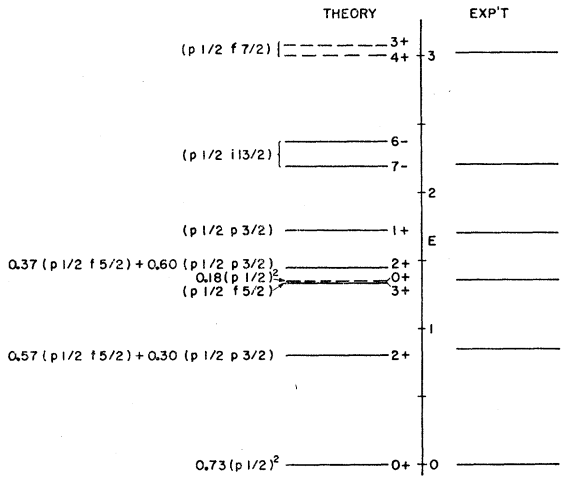

FIG. 7. $Pb^{207}(d,t)Pb^{206}$ experiment. In the left column are the energy levels which should be seen in this experiment, together with predicted *intensities* of $(p_{1/2}j)$ components. Solid levels have been seen by other methods. Dashed levels have not been seen by other methods. In the right column are the energy levels seen by Harvey (Table III, reference g) in this experiment with poor energy resolution. The three dashed levels are based on the theory with singlet plus collective forces (Table XVI).

[39] K. W. Ford and D. L. Hill, *Annual Reviews of Nuclear Science* (Annual Reviews, Inc. Stanford, California, 1955), Vol. 5, p. 46.

[40] L. Wilets, in *Encyclopedia of Physics* (Springer-Verlag, Berlin, to be published), Vol. 38, Part 1.

doublet. The same experiment repeated with high energy resolution could verify configuration assignments of known levels, could fix the position of the 3+ and 4+ levels near 3 Mev, and could discover the position of the 0+ level predicted near 1.3 Mev. [This level should be weakly excited, since it is predicted to be 17% $(p_{1/2})^2$. It may be very close to the 3+, 1 level at 1.34 Mev—see Table XVI—and be difficult to resolve.]

B. $Pb^{206}(n,n')Pb^{206}$

The inelastic neutron scattering experiments of Day *et al.* (Table III, reference f) have revealed several new levels in Pb^{206} not excited in the decay of Bi^{206}. Further similar experiments could possibly detect other predicted levels. A search for the predicted weaker gamma-ray branches following inelastic neutron scattering would also be of great interest in providing information about the wave functions.

An interesting conclusion to be drawn from the experiments of Day *et al.* is that a one-particle selection rule appears to be operating. Only those states are seen which differ from the ground state in the quantum number of one particle. The state at 1.83 Mev is weakly excited and is predicted (if it is 2+) to contain only a rather small admixture of configurations satisfying this selection rule. The higher 0+ states are apparently not excited at all. However, our spin assignments are based on predicted gamma transition rates and are not certain. Further studies of the gamma rays following inelastic neutron scattering would be of interest. Inelastic proton scattering could also reveal new information about Pb^{206}.[41]

Although a great deal of precise experimental information about the low-energy properties of Pb^{206} is available, considerably more should be obtainable. The discovery of the positions of other energy levels up to about 3 Mev, and the discovery of more gamma decay branching ratios, will make possible a more detailed and searching test of theory than is now possible.

VIII. DISCUSSION

We summarize what we regard as the significant conclusions of this work:

(1) A shell model calculation, utilizing the same strength of internucleon force as observed in the two-body system, including configuration mixing with near lying states, ignoring mixing with highly excited configurations, and ignoring effects of nuclear deformation, can successfully predict the energy levels of Pb^{206} up to about 3.2 Mev.

(2) The energy level results are sensitive to (a) zero order positions of the one particle states, (b) strength of the singlet-even force, and (c) strength of collective motion. They are insensitive to (a) strength of the triplet-odd force (within reasonable limits), and (b) radial form of the two-body potential. They are probably rather insensitive to the range of the force and the size of the nucleus.

(3) The measured electric quadrupole transition rate in Pb^{206} can be understood in terms of a weak coupling of the neutron holes to collective quadrupole vibration, with a strength of coupling the same in Pb^{206} as in Pb^{207}.

(4) The agreement between theory and experiment for $M1$ and $E2$ gamma transition rates is improved by the use of mixed state eigenfunctions, but factors of difference as great as 5 remain. The calculated rates are nevertheless very useful in making spin and parity assignments. It is not known whether the failure of precise agreement rests on inaccurate eigenfunctions or on inaccurate transition operators.

(5) If a strength of coupling to collective motion required to account for the measured $E2$ transition rate is included in the energy calculation, agreement with experiment is obtained only for a direct two-body force whose strength is about 75% of the strength for the two-body system at low energy.

(6) The difference in the separation energies of a neutron from Pb^{206} and from Pb^{207} is given approximately correctly by the shell model calculation.

(7) There is no evidence for many-body forces.

That the calculated degree of mixing is approximately correct is indicated in particular by (a) the calculated extra depression of the ground state, which is important for the energy-level agreement, (b) the splitting of the two 4+ states in Pb^{206}, (c) the splitting of the two 4+ states in Pb^{204}, (c) the absolute energy agreement, (d) the agreement with the $Pb^{206}(d,p)Pb^{207}$ cross sections to p states, and, somewhat less reliably, by (e) the fact that the Pb^{206} and Pb^{207} collective coupling strengths are calculated to be equal.

Application of the same model to the nuclei Pb^{205} and Pb^{204} is in progress.

[41] Some interesting inelastic proton scattering results with low-energy resolution have been obtained recently by B. Cohen, [Phys. Rev. **106**, 995 (1957)].